Contemporary and Historical Hydrologic Analysis of the Ballona Creek Watershed

Final Report to the Santa Monica Bay Restoration Commission

Shu-wen (Sharon) Liu
Terri Hogue
Eric D. Stein
Janet Barco



Southern California Coastal Water Research Project

Technical Report 683 - December 2011

Contemporary and Historical Hydrologic Analysis of the Ballona Creek Watershed

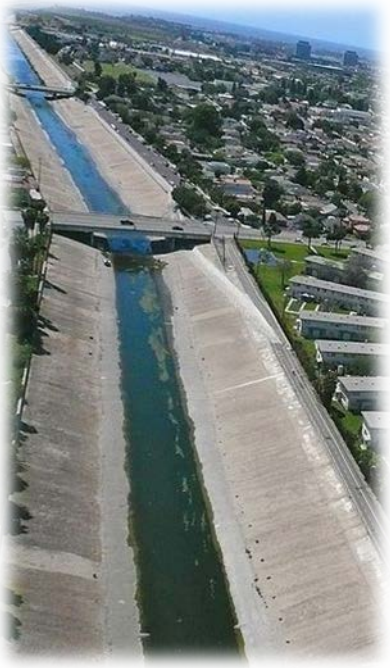

Final Report to the Santa Monica Bay Restoration Commission

December 2011

Shu-wen (Sharon) Liu[1]
Graduate Student Researcher

Terri Hogue[1]
Associate Professor

Eric D. Stein[2]
Principal Scientist

Janet Barco[1,3]
Postdoctoral Researcher

[1] Department of Civil and Environmental Engineering - University of California, Los Angeles

[2] Southern California Coastal Water Research Project (SCCWRP)

[3] Now at Sandia National Laboratories

Table of Contents

List of Figures

List of Tables

Acronyms

AET	Actual Evapotranspiration
BCWMP	Ballona Creek Watershed Management Plan
C-CAP	Coastal Change Analysis Program
CDEC	California Data Exchange Center (Department of Water Resources)
CIMIS	California Irrigation Management and Information System
ε	Residual (represents net water balance errors and uncertainties)
ET	Evapotranspiration (ET_o = reference crop evapotranspiration; ET_{combo} = modified AET + modified PET))
GWAM	Groundwater Augmentation Model
HOBO	Pressure Transducer Gauge
I/Re	Infiltration and recharge (groundwater)
IW	Imported Water
LAA	Los Angeles Aqueduct
LACDPW	Los Angeles County Department of Public Works
LADWP	City of Los Angeles Department of Water and Power
MODIS	Moderate Resolution Imaging Spectroradiometer
MWD	Metropolitan Water District of Southern California
NCDC	National Climatic Data Center
NLCD	National Land Cover Database (USGS)
OWU	Outdoor Water Use
%OU	Percent of Total Residential Water Used for Outdoor Purposes
P	Precipitation
PET	Potential Evapotranspiration
Q	Stream Discharge
R	Surface Runoff
Re	Groundwater Recharge
S	Soil and Groundwater Storage
SPI	Standardized Precipitation Index
TIW	Total Imported Water
WBMWD	West Basin Municipal Water District
ULTRA	Urban Long Term Research Areas
USGS	United States Geological Survey
UWMP	Urban Watershed Management Plan
UWU	Urban Water Use
WY	Water Year (defined as October 1 to September 30, e.g., WY2011 starts on October 1, 2010 and ends on September 30, 2011)

Executive Summary

The current study investigates the partitioning of native and non-native water sources for the Ballona Creek Watershed—a highly urbanized system within the Los Angeles basin. The goal is to evaluate the impact of imported water on spatial and temporal hydrologic cycling and to develop conceptual models of the system as it has evolved from pre-development through the contemporary period. The conceptual model includes precipitation and imported water (outdoor use) as inputs and evapotranspiration, runoff, and groundwater recharge as outputs. The residual term from the water balance accounts for the aggregated uncertainties from model components as well as inputs or outputs that may be unaccounted (leaky pipes, wastewater return, etc.). Daily data were collected and aggregated to the basin-wide annual values for use in the long-term comparison. Components were then analyzed to identify trends and temporal variability. To determine runoff partitioning between native (rainfall) and non-native (imported water) sources, imported water and regional springs was analyzed.

Precipitation throughout the study period has a long-term annual average of 409 mm, with distinct seasonality. January and February are the wettest months, bringing in almost half of the total annual precipitation each year. Annual average runoff for the study period was 204 mm. Runoff ratios (runoff/precipitation ratio) more than doubled during the 73-year study period, increasing from .07 (pre-development) to around 1.0 (contemporary period). The amount of total imported water doubled and outdoor landscape tripled over the 73 year study period. Long-term outdoor water use was estimated at 246 mm. Average evapotranspiration rates were 393 mm during the study period. Annual evapotranspiration peaks during the summer and we hypothesize that the plants are not water limited and precipitation is playing less of a role in vegetation transpiration across the watershed. Water balance results indicate that the sum of recharge and the residual is +58 mm for the most recent period. More work on long-term groundwater table levels is necessary to refine our estimates and reduce the model residual.

For the pre-development period, precipitation was assumed to remain constant (409 mm). Annual runoff was estimated to be 29 mm based on historical irrigation reports, resulting in a runoff ratio of 0.07. Evapotranspiration estimates were based off a water limited scenario so the pre-development annual depth was estimated to be 164 mm. The pre-development water balance estimates the sum of recharge and residual is 216 mm, indicating greater groundwater recharge and potentially larger uncertainties associated with the early water budget estimates, particularly evapotranspiration.

Field measurements were also undertaken to measure sub-watershed runoff and spring flow contribution to runoff. Data was collected at several sites to develop a preliminary understanding of distributed flows in the watershed. Results indicate that sub-watershed area was a good predictor of the percentage flow contribution to the total runoff at the outlet. Extensive field investigations were performed to locate springs based on 41 mapped pre-development springs. The 29 springs which were identified covered approximately 20% of the

total watershed area and had an aggregated flow rate of 0.00057 m^3/s during the dry season. This accounts for 2% of the dry season runoff implying that the remaining 98% was from non-native (imported water) sources.

Differences between the pre- and post-development water balance residuals highlight the anthropogenic impacts on watershed fluxes and the reduction of natural recharge across the basin. Land cover transition from pervious to impervious surfaces governed the water balance evolution and increased both dry and wet season runoff from pre-development to the contemporary period. We estimate the uncertainties associated with our model residual could be as high as 40%, with the largest uncertainty likely related to our evapotranspiration estimates.

Background

Los Angeles, the second most populous city in the United States (US Census, 2000), relies on some of the oldest and most extensive water redistribution projects in the United States. Its large population and semi-arid climate forces it to rely on imported water (IW) from the Sierra Nevada Mountains, the San Joaquin/Sacramento River delta, and the Colorado River for most of its consumptive uses. Allocations from these sources have been declining due to increased concern over the ecological effects of diversion and increased demand from growing urban centers. Increasingly, local governments and water districts in southern California are working towards more dependence on local water sources, including local groundwater, rainwater capture, conservation measures, and recycled water sources. Reliance on local water sources requires more precise understanding of sources, sinks, and uncertainties of water use as a means of more effectively managing available resources. The current project establishes a water budget and investigates the partitioning of native and non-native water sources for the Ballona Creek watershed—a highly urbanized system within the Los Angeles basin. The goal is to evaluate IW impacts on the spatial and temporal hydrologic cycle and to develop conceptual models of the system as it has evolved from pre-development through the contemporary period, accounting for details such as spring contribution, recharge, landscape runoff, spatial evapotranspiration and other hydrologic fluxes. Results from the study will help guide ecosystem restoration in the Ballona Creek watershed and other regional restoration projects.

Study Area

The Ballona Creek watershed is located in the greater Los Angeles basin of southern California. This coastal watershed extends north into the Santa Monica Mountains, west into Beverly Hills and Culver City, east into downtown Los Angeles, and south to the Westchester Bluffs. The majority of the watershed is located in the city of Los Angeles, but the study area also includes Beverly Hills, West Hollywood, unincorporated areas of Los Angeles County, and parts of Culver City and Inglewood. Ballona Creek drains to the Santa Monica Bay with its outlet located adjacent to Marina del Rey. Natural channels remain at the headwaters of Ballona Creek while underground storm drains serve the middle portion of the watershed. The lower portion of Ballona Creek contains concrete-lined channels, either trapezoidal or rectangular-shaped. This study demarcated the terminus of the upper watershed at the existing Army Corps of Engineers/Los Angeles County gauging station, which is approximately 4.8 km (3 mi) upstream of the tidal portion of the channel. The total contributing area of the catchment above the gauging station is 231 km^2 (89 mi^2), where it is 63% residential, 16% commercial/industrial, 2% parks and lawns, and 1% golf courses, making the watershed 82% developed. Average percent impervious values for each developed land use indicate that the watershed is 35% impervious. The remaining area of the watershed includes 10% chaparral, 3% mixed forest, 3% sage, and 2% other. The watershed contains neither dams nor treatment plants.

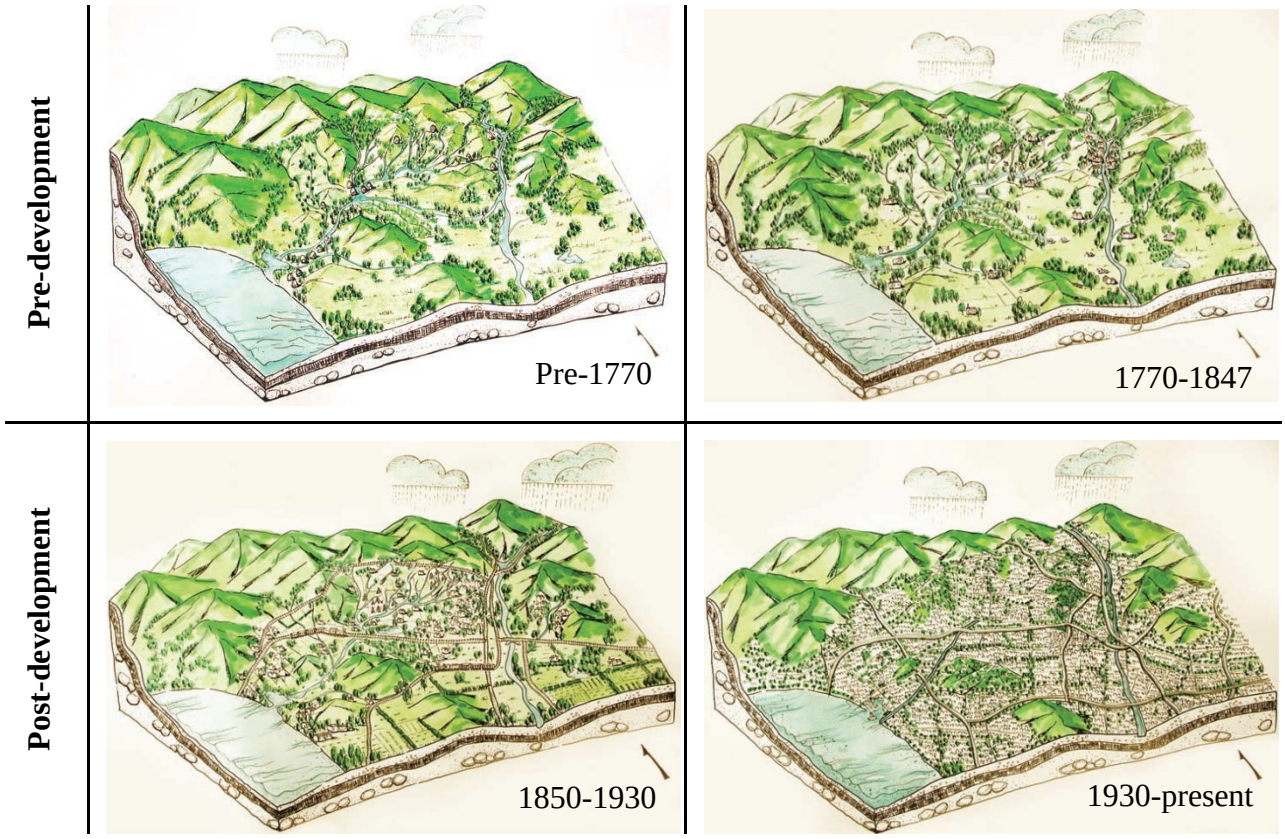

Figure 1: Pre- and Post-Development Depictions of the Ballona Creek Watershed (Braa et al., 2001)

Prior to the 1850s, the Ballona Creek watershed was characterized by a complex drainage network of intermittent and perennial streams in hydrologic connection with springs, seeps, wetlands, and shallow vadose zones (Figure 1). During this period, the neighboring Los Angeles River flowed through what is now considered Ballona Creek until 1825 when a large flood permanently diverted the Los Angeles River to its current outlet. This event substantially reduced the effective area of the Ballona Creek watershed. Shortly after the migration of the Los Angeles River, land uses transitioned from natural cover to agricultural and pasture uses, disrupting the hydrologic cycle by altering runoff rates and pathways, affecting groundwater supplies, and increasing the potential for downstream flooding (Bhaduri et al., 2000). As the population grew in the watershed, more development resulted in increased impervious surfaces. For flood protection purposes, Ballona Creek was channelized from 1935 to 1939 and its tributaries were channelized in the 1950s (SWRCB). Imported water entered the Los Angeles basin in the early 1900s, when natural supplies were unable to meet the demand. The addition of non-native water disrupted the hydrologic cycle by amplifying net water output. Today, the watershed is reliant on IW to fulfill almost all of its water needs.

Current management objectives in Ballona Creek, as described in the Ballona Creek Watershed Management Plan (BCWMP) include water conservation to reduce reliance on IW, water quality treatment to reduce pollutant loading to the coast, and environmental restoration of impaired creeks and the remnant wetlands at the terminus of the watershed (BCWMP, 2004). Meeting these objectives will require improved understanding of the partition between native and non-native water contributing to runoff, identifying long-term water use trends, and pinpointing water balance uncertainties. Identifying watershed fluxes and their related uncertainties will help managers weigh divergent interests in the watershed, such as how to balance coastal water quality concerns with opportunities for stream and wetland habitat restoration.

Methods

The initial phase in the current project involved conceptualizing the watershed as a system by identifying all inputs, outputs, and storage. Next, optimal spatial and temporal coverage was factored into the selection of gauged data sources by considering the maximum number of gauges for each water year. Lastly, spatially distributed datasets were aggregated to daily mean watershed values and used in the final water balance equation.

Conceptual Water Balance Model

Hydrologic processes in the Ballona Creek watershed were divided into external and internal fluxes based on their interaction with the watershed boundary (Figure 2). The top boundary represents the land surface and the bottom boundary represents the interface between the unsaturated and saturated soil zones. This model was applicable to both the pre- and post-development periods. The water balance model focused on the long-term external forcings and how they evolved with urbanization.

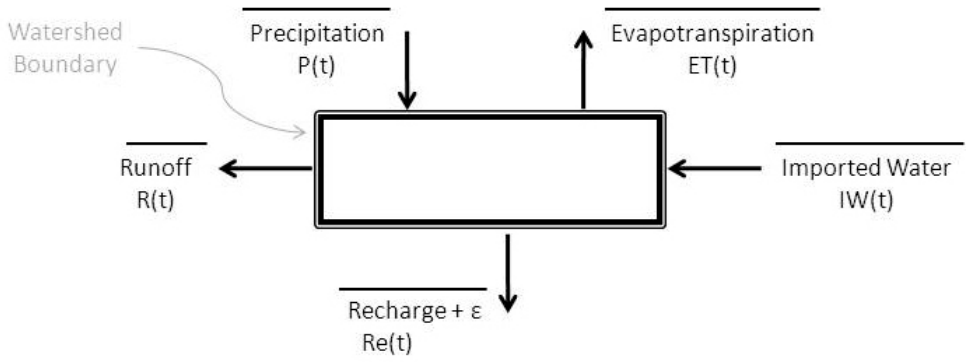

Figure 2: Conceptual Water Balance of the Ballona Creek Watershed (Arrows indicate direction of watershed forcings relative to the watershed boundary; overbars indicate long-term average of water balance components)

A two-dimensional surface water balance with a solvable system of equations is used for this study (control volume approach), using the continuity equation for the general model (Equation 1; Mays, 2005). In Equation 1, $S(t)$ represents the soil and groundwater storage which is constantly variable over short time periods less than a year. The watershed inputs include $P(t)$ for precipitation (P) and $IW(t)$ for the fraction of IW for outdoor uses. Outputs include $ET(t)$ for evapotranspiration (ET), R(t) for surface runoff (R), and $GW_{deep}(t)$ for groundwater recharge (G) through infiltration. The residual (ε) represents net water balance errors and uncertainties. The storage change is assumed zero over the long term (annual cycle in this case). Internal fluxes include the interactions between infiltration, groundwater, and daylighting spring water. The groundwater term considers perennial natural springs and minimal groundwater extraction (pumping).

$$\frac{dS(t)}{dt} = P(t) + IW(t) - ET(t) - R(t) - GW_{deep}(t) + \varepsilon \qquad \textbf{Equation 1}$$

Data Sources and Collection

The study area was delineated from the Los Angeles County streamflow gauging station located in the southwest corner of the watershed (Figure 3). The drainage system was dictated by built infrastructure and was undertaken primarily using the storm drain network. Spatial drainage data used for delineation came from the Los Angeles County Department of Public Works (LACDPW) Spatial Information Library website (LACDPW, 2010). Selecting additional gauged data sources depended on knowledge of the watershed boundary.

Given available daily data sources, the study period was designated from 1938 to 2010 (73 year period). Water balance components were analyzed over complete water year (WY) periods, defined as October 1 of the previous year to September 30 of the designated year, with minimal missing data (less than several consecutive days totaling no more than 30 days out of a year). Missing data was filled through correlations with nearby gauges. Components came from a range of data types and sources; some were from historical gauged data, while others were from contemporary remotely-sensed satellite sources.

The temporal coverage of gauged data varied depending on when the gauges were installed or removed (Figure 3a). Gauges were chosen based on watershed proximity and spatial coverage relative to the others during a specific period(Figure 3b). In all, there was one streamflow discharge gauge, 14 P gauges, five air temperature gauges, and one California Irrigation Management Information System (CIMIS) station for ET estimates. Additionally, several pressure transducers (HOBOs) were installed along the main channel to measure the contribution of major tributaries. Tabulated gauge information is in Appendix A.

a)

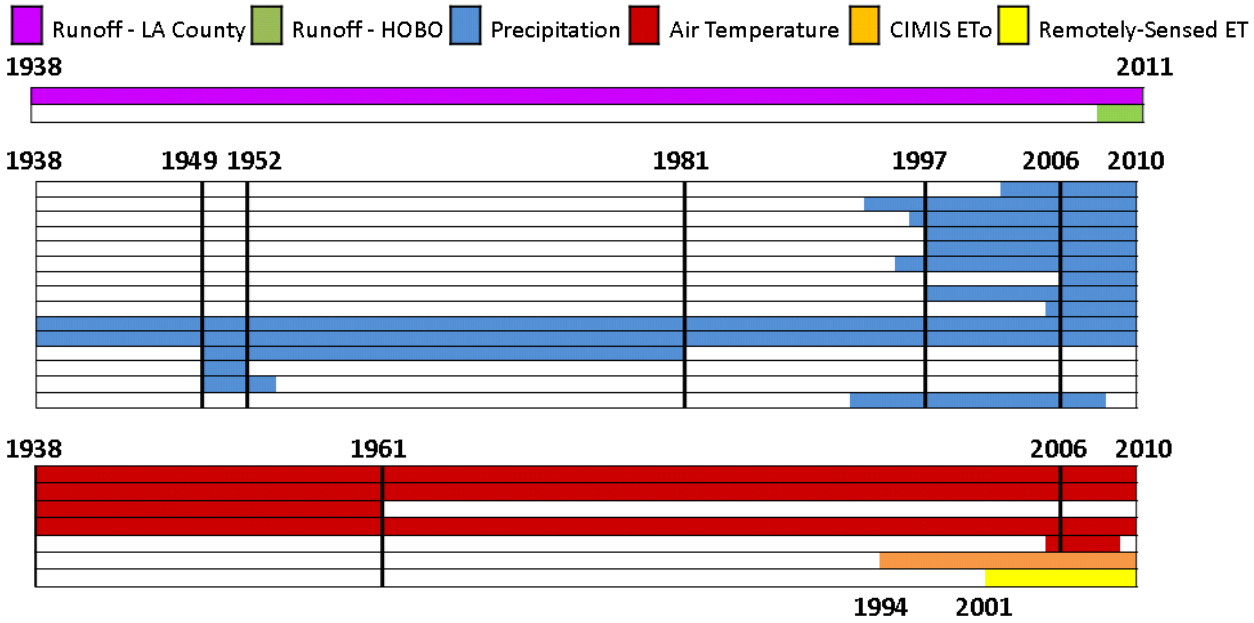

b)

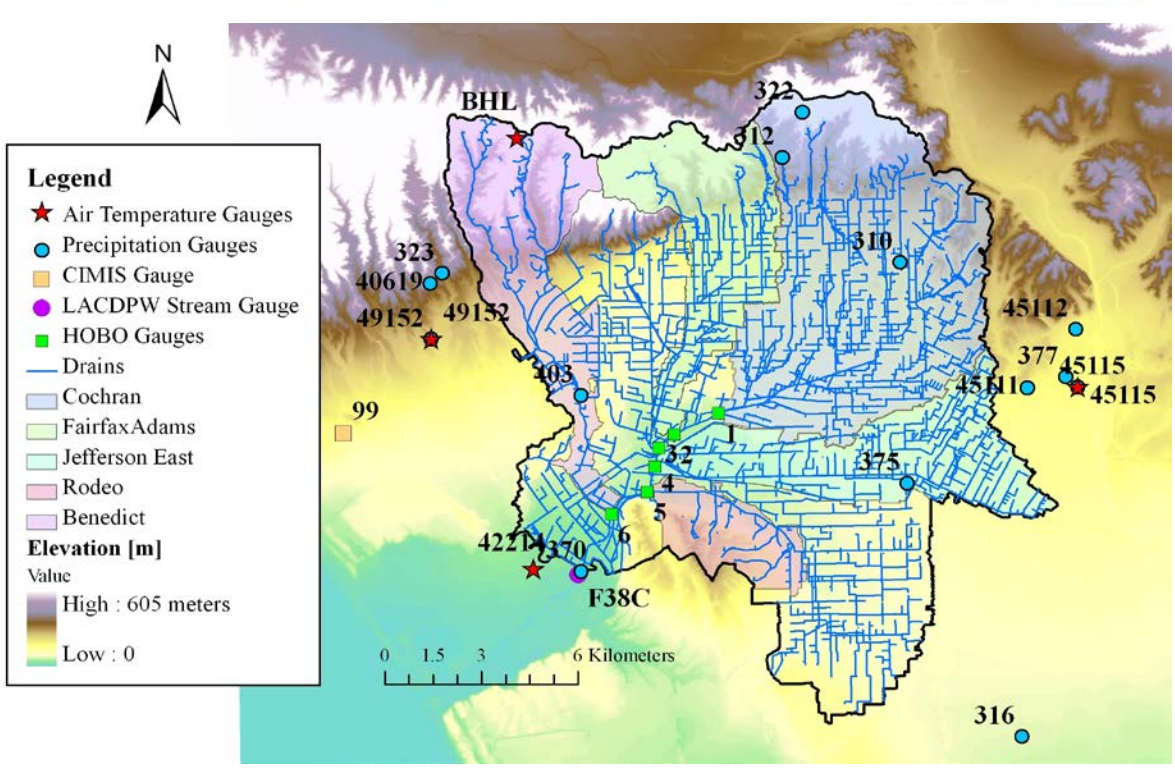

Figure 3: Temporal Coverage by Water Year and Water Balance Component for All Gauges (a) and Spatial Coverage of Data Sources (b)

Tributary Flow Estimates

Nine HOBO pressure transducers were installed to measure flows for six tributaries between November 12, 2009 to March 2, 2011, spanning two wet seasons and one dry season (Figure 3b). Six of the HOBOs were submerged to measure water depth (based on pressure) while three were not submerged to correct for barometric pressure fluctuations. High resolution (5 to 10 minute) data was collected to capture individual tributary runoff characteristics. The first sensor was installed in the uppermost point of the open main channel to measure discharge from the upper watershed, which is currently conveyed through an underground storm drain system. The remaining five submerged sensors were installed at the outlets of major tributaries. Locations were chosen based on spatial coverage and accessibility. Additional site-specific placement criteria included sufficient water level to guarantee continuous submersion and a straight channel upstream; both were necessary to sustain quality flow estimates. HOBOs were installed at the center of each channel underneath protective metal housings bolted to the channel bottom.

The HOBO data loggers provided measurements of absolute pressure and temperature, which were used to calculate water depth. Based on the cross-sectional dimensions of the concrete channels, surveyed channel slopes, and empirical roughness coefficients, rating curves were developed using Manning's Equation (Equation 2) and discharge was estimated based on stage height (water depth). The HOBO sensors were set to measure at 5-minute resolution during the wet season and 10-minute resolution during the dry season when there was less variability. During each site visit (approximately every 56 days) flow rates were measured for use in rating curve development. Uncalibrated and calibrated rating curves were created using Manning's Equation. The uncalibrated rating curve was calculated based on measured dimensions and a standard channel roughness for concrete of 0.015 (Chow, 1959). The uncalibrated rating curve was then calibrated to match field measurements of flow and depth by adjusting Manning's *n*. A major limitation was the lack of high flow values for calibration, resulting in relatively high sensitivity to equation parameters. Additional details can be found in Appendix B.

$$Q = \frac{1.49 A R^{2/3} S^{1/2}}{n} \qquad \textbf{Equation 2}$$

Where Q is stream discharge (ft^3/s), A is cross-sectional area (ft^2), R is the hydraulic radius (ft) (or cross-sectional area/wetted perimeter), S is channel slope, and n is Manning's roughness coefficient.

Missing Data

Air temperature and wind speed were assumed to generally behave linearly over time. Based on this assumption, missing data values were filled using a linear interpolation. This simplified method was chosen because consecutive days with missing data were limited. Precipitation data sometimes had periods of missing data exceeding a two-week period, therefore

a more sophisticated estimation method was necessary. Gauges with missing data were compared with all other gauges to determine the similarity using Pearson's correlation coefficient. The gauge with the highest correlation to the gauge lacking data was used to fill missing data using a linear regression.

Data Aggregation

For each component, daily data from several gauges was aggregated using the Thiessen Polygon method to produce a mean areal value for the entire watershed (see Appendix A and B). Daily watershed values for each component were then summed or averaged to obtain monthly or yearly values.

Calculations

Impervious and Pervious Area

Using the 1992 (NLCD) and 2001 (C-CAP) land cover maps, the watershed area was partitioned into three types: impervious, pervious with limited water, and pervious with unlimited water. Percentage impervious area was calculated from land cover data and impervious fractions for specific land covers in the 2006 LACDPW Hydrology Manual (LACDPW, 2006). Impervious surfaces include buildings, roadways, sidewalks, etc. Water-limited areas include all natural areas that rely on P input such as chaparral, sage, mixed forest, etc. Areas with unlimited water include open water surfaces such as lakes and reservoirs and also irrigated areas which are well-watered and transpire at potential levels. Values were back-filled using a linear regression with the estimated watershed population.

Water Year Classification

The Standardized Precipitation Index (SPI) was used to classify water years into wet, normal, and dry. The SPI was developed as a drought planning tool in 1993 by McKee, Doesken, and Kleist at Colorado State University (McKee et al., 1993). The SPI is used to calculate the probability of P during a user-specified time-scale by normalizing the data and calculating a standard deviation from the mean. The calculation requires >30 years of monthly P data and outputs a monthly SPI value (SPI > 1 [wet], -1<SPI<1 [normal], and SPI < 1 [dry]). For this project, a season was defined as one water year (or a 12-month period).

Imported Water

Imported water was divided into indoor and outdoor uses. Only outdoor water use (OWU) impacts the water balance because water physically penetrates the watershed boundary and contributes to ET, R, and infiltration as opposed to indoor water use which goes to the sanitary sewer system. The Outdoor water use was modeled using the Hydrologic Region method developed by the Pacific Institute (Gleick et al., 2003):

$$OWU = pop \times UWU \times \%A_{\text{urb.res.}} \times \%OU \qquad \textbf{Equation 3}$$

Where *pop* refers to the population, *UWU* refers to urban water use (UWU) which represents the total amount of water use excluding recycled water, $\%A_{\text{urb.res.}}$ is a percentage of total watershed area that is urban residential, and $\%OU$ is the percent of total residential water use that is for outdoor purposes.

Based on the availability of data, the annual composite OWU was calculated from the three water providers. Population data for each city came from the U.S. Census Bureau and UWU values came from respective water providers. To calculate the population within the Ballona Creek watershed, zip code resolution population data was plotted and the total population was extracted from the 2000 U.S. Census. Assuming uniform population distribution, zip codes partially inside the watershed were reduced relative to its area inside. Similarly, for other years, city population data was scaled by its area inside the watershed. Percentage urban residential was calculated for 1992 and 2001 using U.S. Geological Survey's (USGS) National Land Cover Database (NLCD) and California C-CAP, respectively. Using these two data points, a linear regression was performed to backfill historical values. Percentage OWU was calculated for each water provider's area using the city of Los Angeles Department of Water and Power (LADWP) Urban Watershed Management Plan (UWMP) published values for major land usages including single-family, multi-family, commercial, industrial, and government (LADWP, 2010). Using land cover data, a weighted %OU value was created for each water provider.

Evapotranspiration

Evapotranspiration is the combination of the evaporation and transpiration processes. There are three different types of ET: potential evapotranspiration (PET), reference crop evapotranspiration (ET_o), and actual evapotranspiration (AET). The PET estimates the maximum possible amount of evaporative loss over a uniformly vegetated area assuming that there is an unlimited water supply. Calculations often depend on measured meteorological parameters such as air temperature, relative humidity, and solar radiation. The ET_o measures the PET of a specific crop. The AET estimates the real amount of loss due to a limited amount of water. This study utilized ground-based climate data to estimate ET for the entire study period and a remotely-sensed algorithm (Kim and Hogue, 2008) for comparison during WY2006.

All selected PET methods are a function of air temperature while AET methods are a function of P and PET. Common methods were utilized, including: Schrieber (1904), Ol'dekop (1911), Hargreaves (1947), Thornthwaite (1948), Turc (1954), Blaney and Criddle (1962), and Budyko (1974). For comparison, ET_o values from the nearby Santa Monica CIMIS station were used. Evapotranspiration was calculated for each air temperature gauge before it was aggregated using the Thiessen Polygon method. Equations for each method are in Appendix B, and a summary is provided in Table 1.

Table 1: Ground-Based Evapotranspiration Methods

Method	Type	Variables
Blaney-Criddle	ET_o (cm/month)	f(T_a, K, d, grass surface) K = empirical crop factor d = fraction of annual hours of daylight for the month
Hargreaves	PET (mm/day)	f(T_a, S_o, δ_T, grass surface) S_o = water equivalent of extraterrestrial solar radiation (mm/day), f(latitude, Julian day) δ_T = change in daily minimum and maximum air temperature (°C)
Thornthwaite	PET (mm/month)	f(T_a, b) b = monthly adjustment factor related to hours of daylight
Budyko Ol'dekop Schreiber Turc	AET (mm/period)	f(PET,P) P = precipitation (mm)

Results

Results from each component of the water balance are presented below.

Precipitation

Fourteen gauges were selected based on gauge availability over the study period (Figure 1). Periods of record for each gauge varied; hence, eight sub-periods were used within the overall study period WY1938-1948 (2 gauges), WY1949-1951 (5 gauges), WY1952-1980 (3 gauges), WY1981-1996 (2 gauges), WY1997-2005 (8 gauges), WY2006-2008 (11 gauges), WY2009 (10 gauges), and WY2010 (9 gauges). Thiessen Polygon weights were developed based on the number of gauges per sub-period (shown in parentheses) and their spatial distribution.

The long-term annual average P in the watershed is 409 mm (16.1 in). During the study period, the driest year was WY2007 with 86 mm (3.4 in) and the wettest year was WY2005 with 933 mm (36.7 in). The long-term annual monthly averages (Figure 10) show distinct seasonality with January and February being the wettest months of the year with values of 88 mm (3.5 in) and 97 mm (3.8 in) average values, respectively. The summer season (June, July, and August) averages <3.7 mm (0.15 in) of P.

The SPI indicates that there were 9 wet, 58 normal, and 6 dry years (Figure 4). The wet water years were: 1941, 1969, 1978, 1979, 1980, 1983, 1993, 1998, and 2005. The dry water

years were: 1949, 1951, 1961, 1990, 2002, and 2007. All other years during the study period were normal water years.

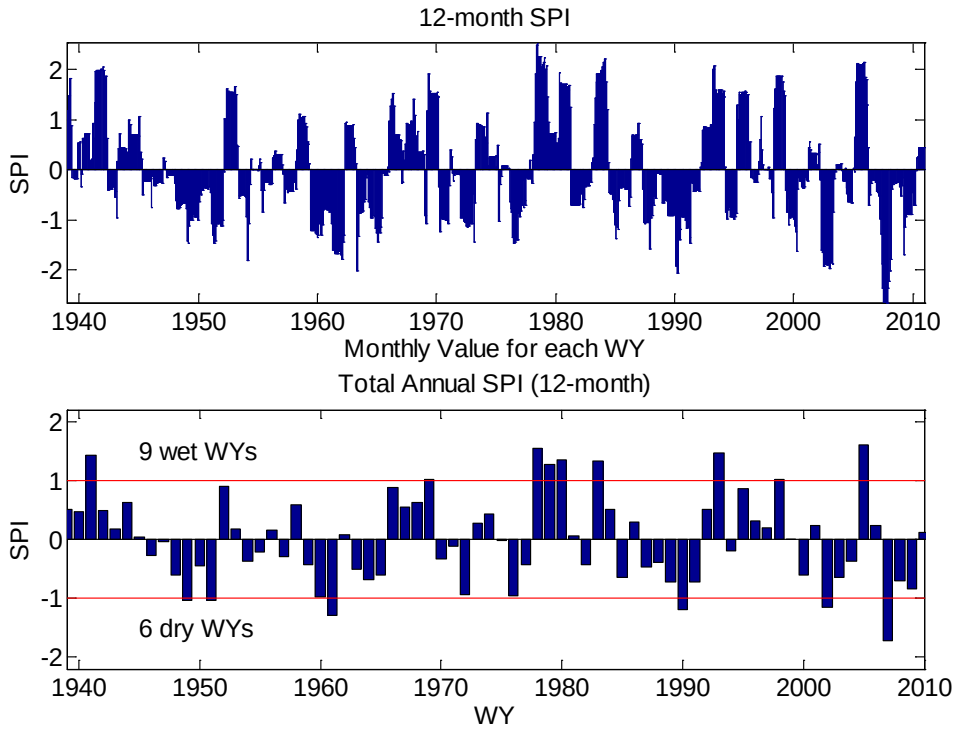

(Top: monthly SPI values, Bottom: aggregated annual SPI values)

Figure 4: Monthly and Annual Standardized Precipitation Index (SPI) for WY 1939-2010

Runoff

Both total watershed and distributed (sub-watershed) runoff were studied. The gauging station at the outlet of the watershed measures the entire watershed's runoff and HOBO pressure transducers were used to estimate sub-watershed runoff. Runoff depths were calculated by dividing flow rates by the respective area above each gauge.

Watershed Scale

Both native (P) and non-native (IW) sources contribute to R in urban systems. Annual R results indicated that the long-term average R depth was 204 mm (8.0 in). WY 2005 had the greatest flow with 705 mm (27.8 in) which corresponded to the wettest year. On the other hand, WY 1961 only had 67mm (2.6 in) of flow because it was a dry year with only 104 mm (4.1 in) of P. Although WY 2007 was actually the driest study year, it had 79 mm (3.1 in) more R than WY 1961. The population grew by 50% between 1961 and 2007 likely increasing R due to IW.

Annual R ratios (R/P) were calculated by dividing R depth by P depth (Figure 5). An increasing trend over time was observed with considerable variability occurring after 1990. The

increasing R/P ratio is a characteristic of increasing development (Weng, 2001). An R/P ratio of 1 marks the theoretical maximum in natural systems because R (output) cannot exceed P (input); however, in urban systems, IW may cause the R ratio to exceed 1. A combination of below average P and high urban R (landscape irrigation) caused the R/P ratio to exceed the threshold three times during the last decade.

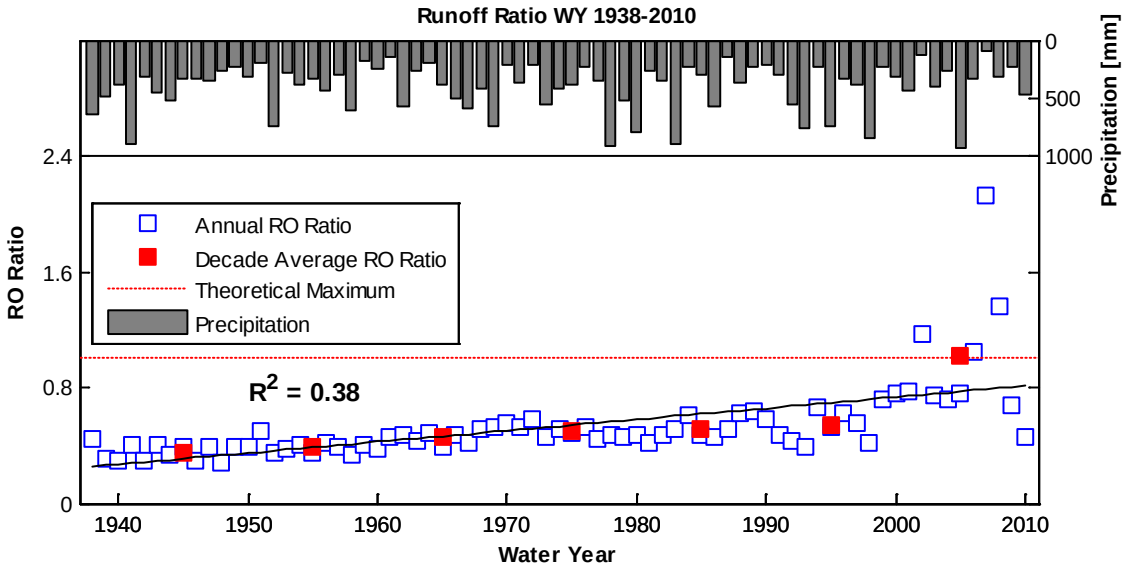

Figure 5: Annual Runoff Ratio (R/P) for WY1938-2010

On a monthly time-scale, long-term averages indicate that the greatest flows occurred in January with 50 mm (2.0 in) and February with 64 mm (2.5 in). The summer season (June, July, and August) produced a total of 19 mm (0.7 in) which was more than five times the amount of P. This additional dry season R was likely from R due to IW (excess landscape irrigation) and perennial spring flows. The partition between these R contributors was not consistent through time.

In-depth R and P interactions were explored using decade average annual cycles from the 1940s to the 2000s (Figure 6). Results indicate that R was less than P during the wet season, but R was greater than P during the dry season (except the 1940s). Although the annual difference between P and R was not significant through the decades, it is hypothesized that R sources had transitioned from native sources to non-native sources, but the exact partition between these sources is unknown. The 1940s did not follow this trend because it was uncharacteristically wet with P exceeding 200 mm (7.9 in) during several months.

Using pre-development irrigation reports (Hall, 1888), early annual R was observed as 29 mm (1.1 in). Assuming P is consistent between pre-development and post-development periods (409 mm) a R ratio of 0.07 is estimated for the pre-development period. Similar R ratios have been reported for undeveloped semi-arid regions, including 0.13 (desert; Nash and Gleick, 1991), 0.103 (rangeland; Chauvin et al., 2011), and 0.12 (chaparral; Hogue, 2009).

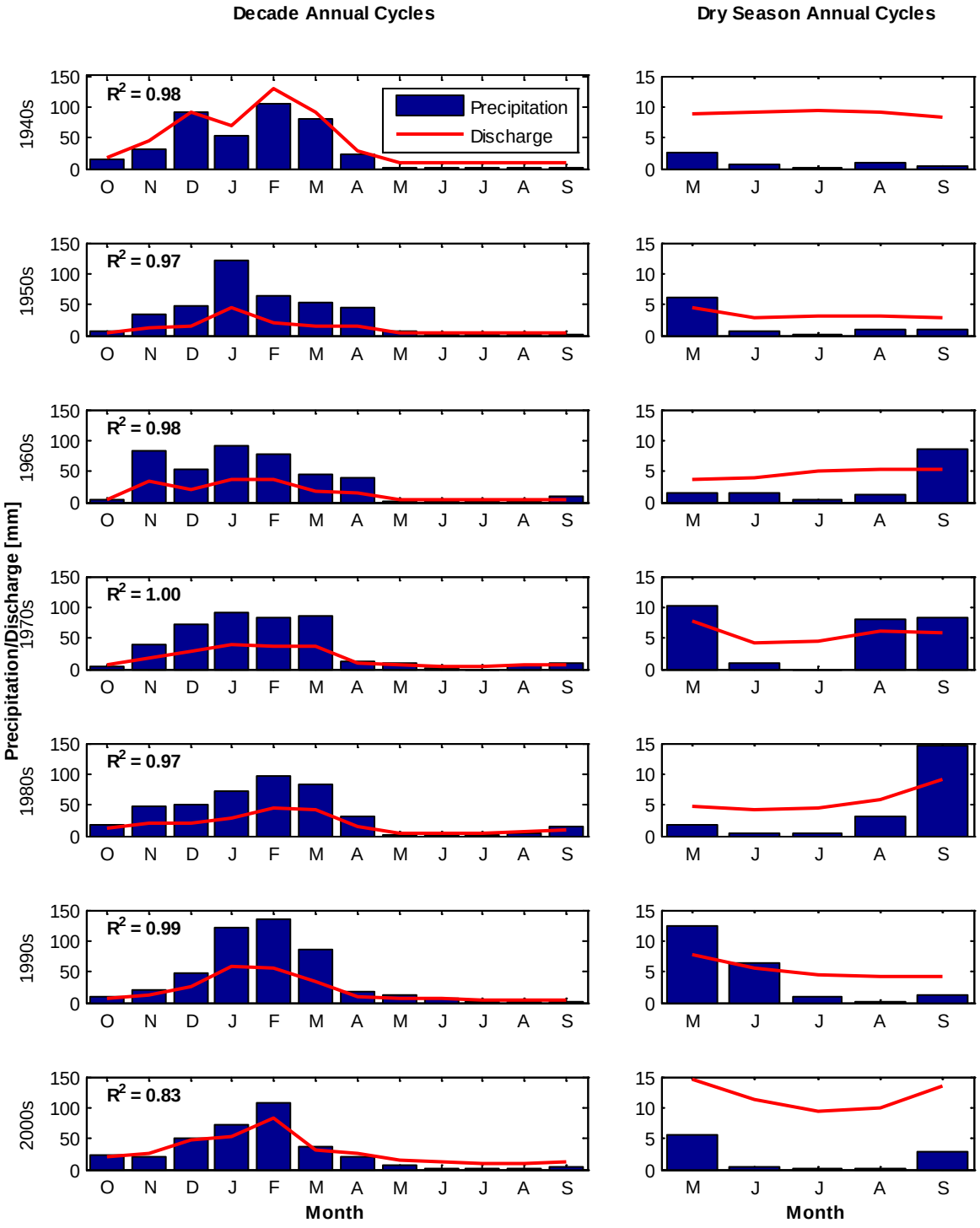

Figure 6: Average Annual and Dry Season Precipitation and Runoff Cycles for Each Decade (e.g., 2000s includes the period from 2000 to 2009)

Sub-watershed Scale

The spatial variability of land use in the Ballona Creek watershed influences the spatial distribution of R sources (Table 2). The gauged sub-watershed areas combine to cover 57% of the total watershed area. The largest sub-watershed was Cochran (#1) and the smallest sub-watershed was Rodeo (#5). The complex drainage network and the flow directions between Fairfax (#2) and Adams (#3) made it difficult to delineate the catchments; therefore, they were analyzed together. Catchment area was linearly correlated with the percentage contribution to total R during high flows, which is expected for the unregulated urban watersheds. Manning's roughness, *n*, for concrete in the calibrated rating curves were unrealistic ranging from 0.0075 to 0.15; thus, uncalibrated rating curves were ultimately chosen for the sub-watershed flow estimates.

Table 2: HOBO Location, Sub-Watershed Area, and % Impervious Area

ID	Location Name	Area (km^2)	% of Total Area	% Impervious
1	Cochran	66	29%	39%
2/3	Fairfax/Adams	26	11%	27%
4	Jefferson	27	12%	53%
5	Rodeo	11	5%	28%
	HOBO Total	*160*	*57%*	*39%*
	Watershed Total	*231*		*35%*

Results indicated that the HOBOs had difficulty capturing the extremes (low and high flows; Figure 7). During low flows (interstorm periods), sensors were often not fully submerged. As a result, low flows were overestimated and high flows were underestimated. Estimation uncertainties are also attributed to rating curve quality, which are particularly noticeable in low flow estimations where errors are magnified. See Appendix C for a full time-series plot. The sub-watershed R results served as an initial step in distributed R analysis and were not used for the annual water balance; however, they provide insight on potential sub-watershed behavior.

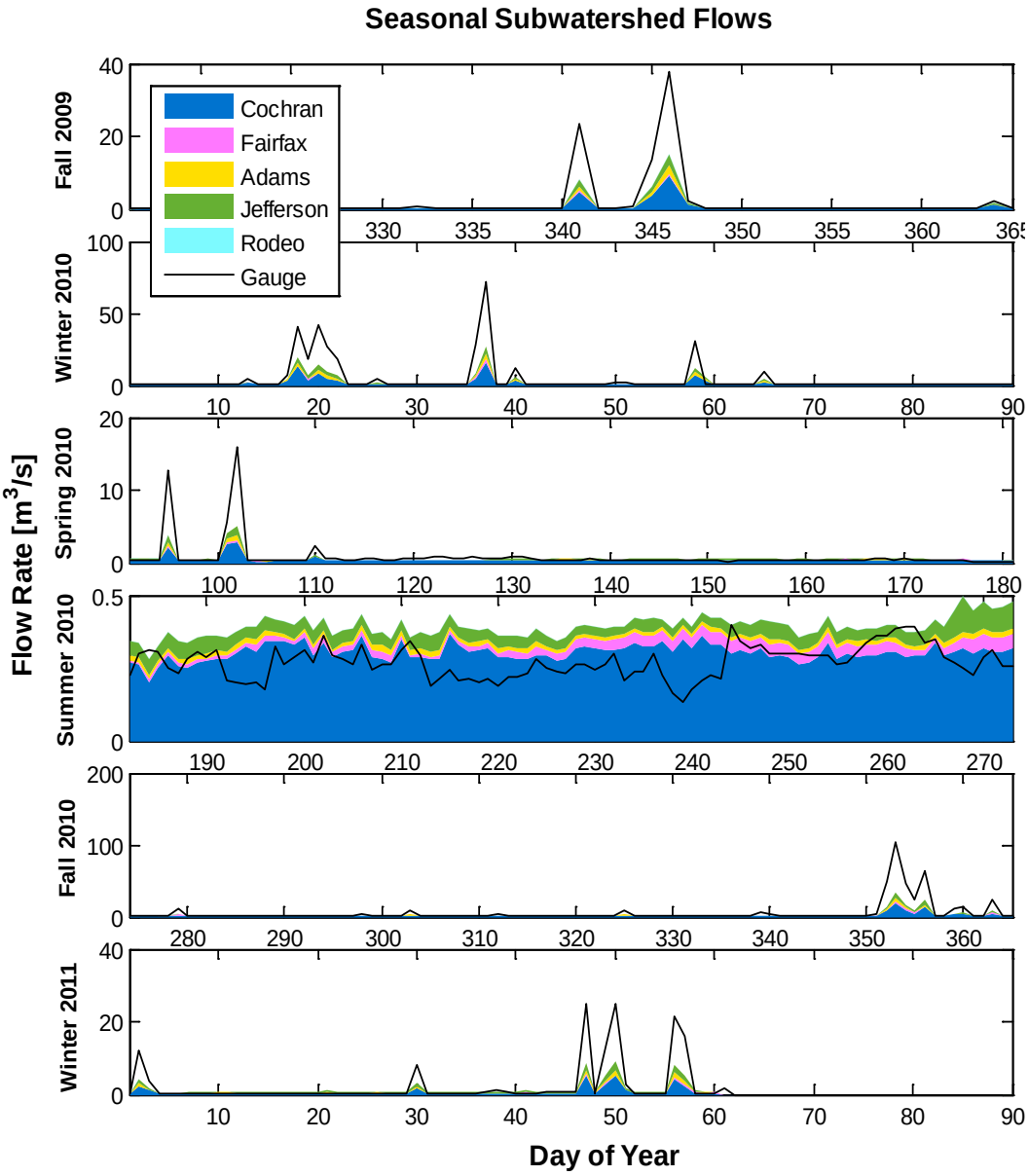

Figure 7: Seasonal Sub-watershed Flow Contribution to Total Daily Runoff (aggregated from 5- to 10-minute resolution data).

Imported Water

Ballona Creek watershed's IW comes from both the Los Angeles Aqueduct (LAA) and the Metropolitan Water District of Southern California (MWD). There are three local water providers for the Ballona Creek watershed (by area): LADWP (91%), Beverly Hills Department of Public Works (4%), and the West Basin Municipal Water District (WBMWD; 5%). Total imported water (TIW) was estimated by scaling down annual total water use for each water provider using the percentage area of the watershed in the service area (Figure 8). This assumed

a uniform water use distribution in each service area. LADWP had the longest record of total water use, thus this data was used to calculate TIW for the other 9% of people whenever data was missing, specifically prior to 1970 and 1979 (panels B and C, respectively, in Figure 8). Precipitation data prior to 1938 (panel A in Figure 8) represents a period with only one gauge and thus the data is only provided for reference.

The average OWU to TIW ratio for Ballona Creek from 1920 to 2010 was 0.31 which was similar to the Pacific Institute's findings of 0.34 for the South Coast Hydrologic Region (Gleick et al., 2003; Heberger, 2009; Figure 8). It was hypothesized that landscape irrigation accounted for most of all OWUs, thus the amount of irrigated area controlled inter-annual total water use variability because indoor water use was assumed to be independent of climate variability.

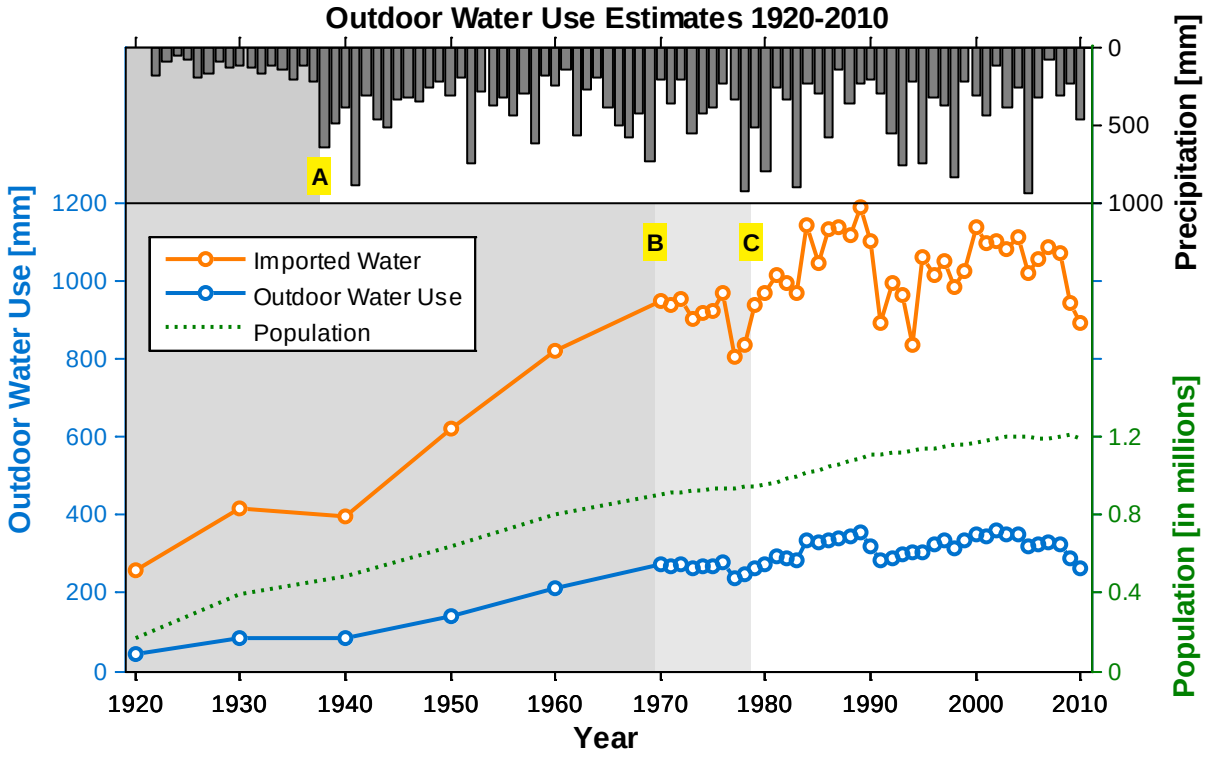

Note: Higher uncertainty is expected prior to: 1938 (A) - only one precipitation gauge, 1970 (B)- lack of Beverly Hills total water use data, and 1979 (C)- lack of West Basin MWD total water use data.

Figure 8: Outdoor Water Use and Population Estimates for WY1920-2010

Infiltration and Recharge

Two surface water sources contribute to infiltration and recharge. These were divided by point of entry, either at the ground surface or underground, and source type, either natural (P) or non-natural (IW). The ground surface was further divided into pervious and impervious areas. Precipitation was the only natural infiltration and recharge source, contributing only at pervious

regions. This included the undeveloped areas in the upper reaches of the watershed and the pervious areas of developed land uses. Imported water was the source of non-natural infiltration and recharge when used outdoors and where leaks have occurred. Regular landscape irrigation in pervious areas maintained high soil moisture levels some of which percolated and contributed to Re. Leaky reservoirs and swimming pools were both potential contributing sources at the surface, while leaky pipelines contributed underground. Water main and sewer line leakages are prevalent in urban areas due to aging pipe infrastructure (Garcia-Fresca, 2005). In Southern California, model results demonstrate that urbanization has decreased natural recharge (He and Hogue, 2011), implying that groundwater aquifers may have a corresponding increase in artificial recharge.

Natural Springs

Dry season runoff had two distinct contributors: natural springs and urban runoff. Natural sources were further broken down into P-driven direct runoff and time-lagged sources. This partition was investigated through natural spring measurements as distinguished by areas with no uphill development as to eliminate non-native water from sources such as irrigation and leaky pipes.

There were at least 41 natural springs mapped in the Ballona Creek watershed prior to development (Dark et al., 2011). Field investigation efforts focused on finding historical springs and estimating dry season discharge. Twenty-nine springs were identified and classified into two categories based on the location of the measurement whether it was from a natural or diverted source (Figure 9). Six natural springs were found in undeveloped parks along the urban fringe, and 17 springs appeared to be diverted from their source through pipes and culverts. The remaining six springs were unmeasured due to access issues, which included: unsafe conditions (e.g., steep terrain), private property, a physical barrier (e.g., grate), or its intermittent nature.

Springs were measured using an electronic flow meter whenever possible; otherwise, measurements were done using a simple bag test to measure a volume capture over a specified time. Most of the measurements were performed during the dry season. The average springs flow rate measured in July 2011 was 0.00057 m^3/s (0.02 cfs). See Appendix C. Assuming there were 20 natural springs flowing at the average rate measured in July 2011, we estimate a monthly depth of 0.13 mm (0.005 in; or 2% of R during July 2011). There was no P recorded in July 2011 (and no direct R), therefore by deduction, the remaining 98% was estimated to come from excess landscape irrigation or human activities. The annual and wet season partitioning between springs sources were different because rainfall was a factor. Slightly higher springs contribution to R is expected during the inter-storm wet periods. However, if dry season rates are scaled up to a year, the baseflow contribution of springs would account for 0.5% of the total annual R which meant the remaining 99.5% would come from non-native sources. We hypothesize that this is a conservative estimate of springs contribution to R because rainfall driven R is expected to hold a much greater proportion.

Pre- Development Springs

(Pre-1850s)

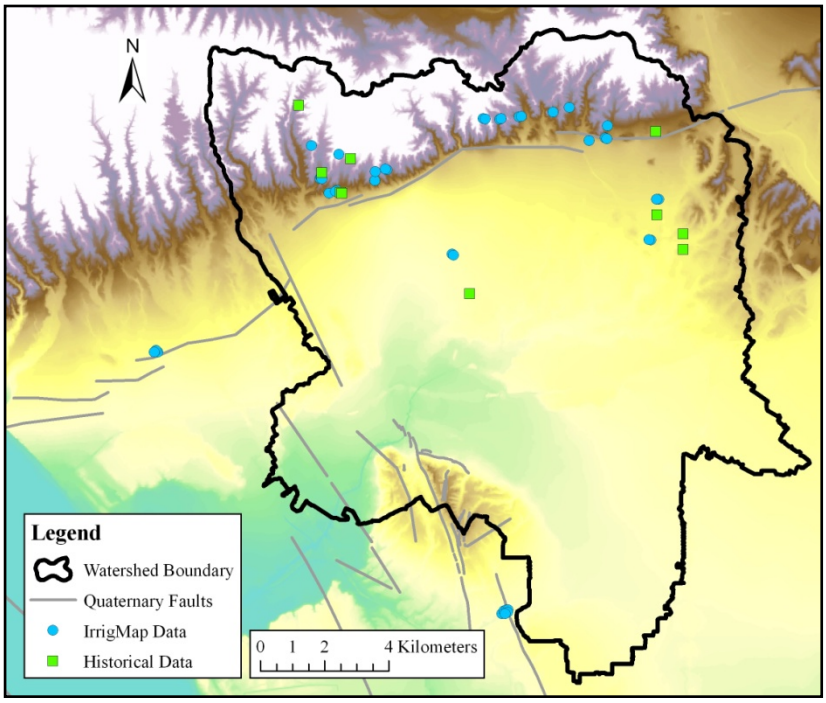

Post-Development Springs

(2011)

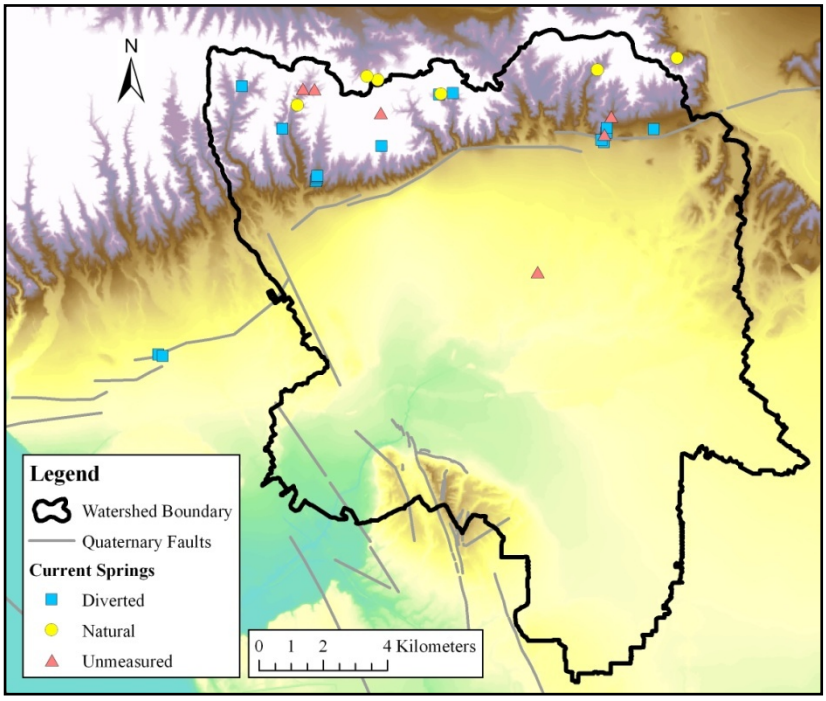

Figure 9: Historical and Current Natural Springs -Top: Historical Springs (Dark et al., 2011), Bottom: Contemporary Springs

To gain insight on the variability in springs, similar estimates were performed on other years during the study period with a similar amount of P (Table 3). Assuming dry season springs flow rates remained consistent between the pre- and post-development periods, the number of springs were scaled up to annual values based on a direct proportionality between the percentage pervious area and the number of springs. This represented the annual spring contribution to baseflow. For the pre-development period, it was assumed that dry season spring flow equaled dry season R. Hall's irrigation report (1888) estimates the average dry season R rate as 24 mm (0.9 in). Dividing this by 41 known pre-development springs yields an average dry season flow rate of 0.59 mm (0.15 cfs) per spring, which indicates that there has been more than a seven fold decrease in dry season flow rates.

Table 3: Estimating Annual Natural Spring Contribution to Baseflow

WY	% Imp	Annual				Springs		% of Annual Runoff	
		ET_{combo} [mm]	Precip. [mm]	Runoff [mm]	Runoff Ratio	# of Springs	Annual Depth [mm]	Contribution of Spring Runoff	Direct + Urban Runoff
2011	0.35	451	465	294	0.61	20	1.55	0.5%	99.5%
2001	0.35	418	435	334	0.77	20†	1.55	0.5%	99.5%
1956	0.26	333	437	185	0.42	23†	1.76	1.0%	99.0%
1939	0.19	199	486	156	0.32	25†	1.93	1.2%	98.8%
Pre-dev	0	164*	409**	29^	0.07	41‡	24.2^^	100%	0%

Notes: * = $ET_{combo} = AET_{avg}$ because $A_{natural} = A_{WS}$ in the ET_{combo} equation
** = Long-term mean from WY1938-2010
^ = average pre-development runoff based on an irrigation report by Hall, 1888.
† = calculated as the # of springs being directly proportional to (1-%imp)
‡ = # of springs mapped by Dark et al., 2011.
^^ = dry season runoff rate from Hall, 1888 (assumed to represent spring flow)

Evapotranspiration

Annual evapotranspiration results are summarized and shown as monthly cycles averaged over multiple years (Figure 10). The PET methods follow the annual air temperature cycle and AET methods follow the annual P cycle. Greater solar radiation input during the summer months (July, August, September) led to higher air temperatures and the vice versa during the winter months (January, February, March). CIMIS and Hargreaves methods showed very similar results, while the Blaney-Criddle method had higher values during the summer season and lower values during winter and spring. The Thornthwaite method produced results similar to the Blaney-Criddle method during the two wettest months (January and February); however, all other months had significantly less ET. Since these methods assumed a fully vegetated area,

which is not the case in Ballona, the lowest PET estimation was the most conservative, thus it was used to calculate AET. As a result, the four AET methods had very comparable values, so only the average of the four AET methods was plotted.

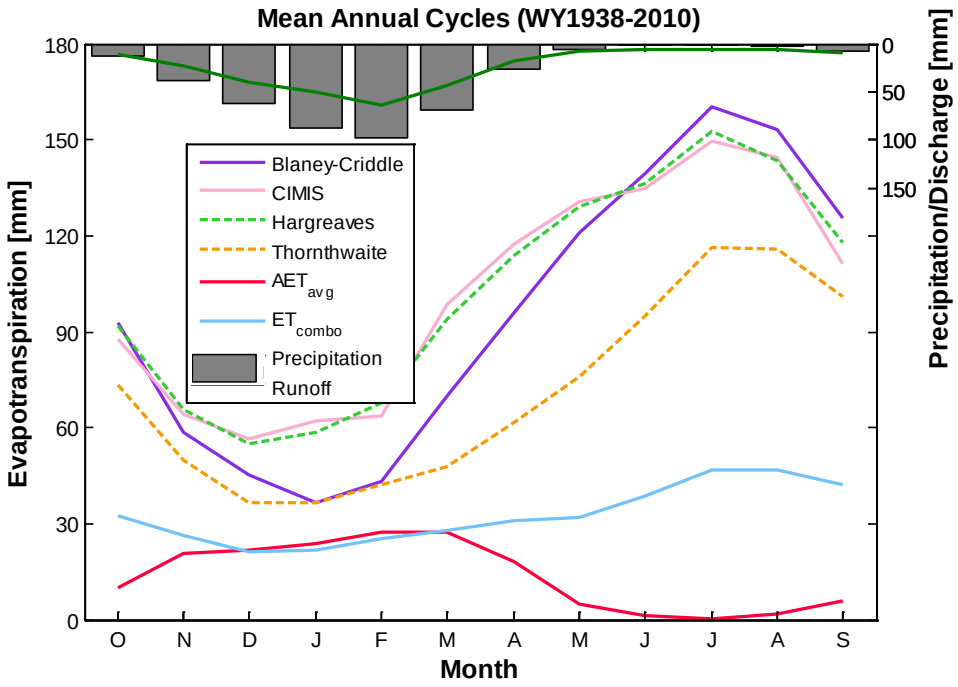

Figure 10: Long-term Monthly Average Annual Ground-Based PET and AET Estimates

It was determined that neither PET nor AET alone accurately represents the true ET in an urban watershed. Using a mean PET value may overestimate ET by assuming the entire watershed area is vegetated and is transpiring at the maximum rate. A mean AET may underestimate because it does not account for well-irrigated areas. We therefore used a combination method (ET_{combo}) with both PET and AET, as described in Equation 4, to address these issues.

$$ET_{combo}[mm/period] = \frac{A_{\text{limited}}}{A_{WS}} \times AET_{avg} + \frac{A_{\text{unlimited}}}{A_{WS}} \times PET \qquad \textbf{Equation 4}$$

Where A_{limited} is the area of the watershed with limited water supply (natural areas), $A_{\text{unlimited}}$ is the area of the watershed with unlimited water supply (landscaped areas), A_{WS} is the total watershed area, AET_{avg} is the annual average of the Budyko, Ol'dekop, Schreiber, and Turc methods, and PET is the annual Thornthwaite value. See Figure 18 for the area breakdown.

Results indicate that the increasing trend in ET_{combo} over the study period was heavily influenced by the land use transition from natural surfaces to impervious and irrigated surfaces

(Figure 11). Ground-based methods only provide point estimates and are unable to capture the spatial variability of ET, so a remote-sensing ET algorithm developed at UCLA was used to calculate daily ET at a 250 m grid resolution (Kim and Hogue, 2008). High resolution ET estimates employed several types of remotely-sensed data from the Moderate Resolution Imaging Spectroradiometer (MODIS) satellite such as land surface temperature, albedo, cloud cover, and vegetation indices. Data was available from 1999 to present for the Terra platform and from 2002 to present from the Aqua platform. The temporal resolution varied between daily, 8-day, and 16-day resolution, and the spatial resolution varied between 30 m, 250 m, and 1 km. MODIS product details are provided in Appendix A.

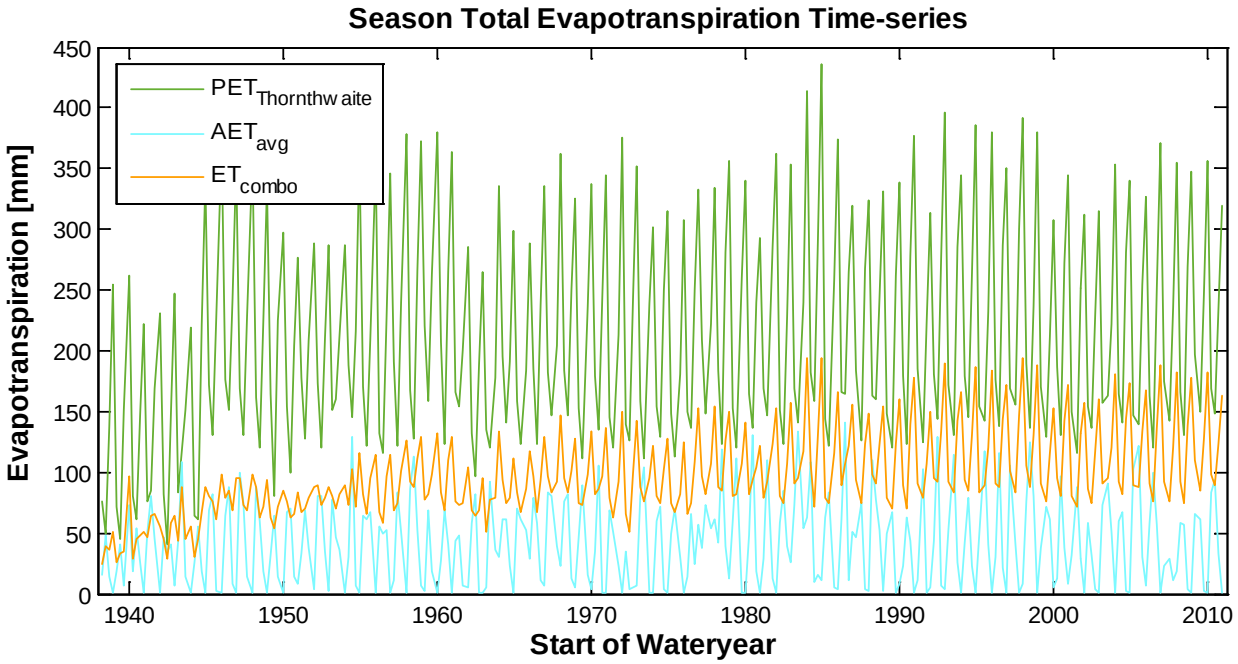

Figure 11: Seasonal Total Evapotranspiration Time-series for WY 1938-2010

To compare ground-based estimates with remotely-sensed estimates, a "normal" wetness water year was chosen using the SPI index (WY2006 with SPI index of 0.24). Daily results are shown in Figure 12 and the monthly time-series comparison in Figure 13. Results indicated that ET during the dry season was greater than during the wet season because of the heavily irrigated landscaped area and the high solar input which provided the necessary resources to drive the photosynthesis process thus resulting in more ET. More ET occurred during the summer despite the lack of P input, which showed that irrigation had a more dominant role than P over the entire year. During the wet season, ephemeral ET spikes were recorded immediately following storm events. The total annual depth of ET estimated was 863 mm (34 in).

Both ground-based and remotely-sensed ET estimates were compared using monthly annual cycles (Figure 13). Results indicated that the Thornthwaite method for estimating PET

best matched the remotely-sensed results for the 2006 period. This confirmed our hypothesis that the Ballona Creek watershed is transpiring at near its maximum potential rate during the contemporary period. In fact, the dry season ET estimate exceeded the "maximum potential" as defined by Thornthwaite (1948); however, the wet season ET did not quite meet the maximum potential.

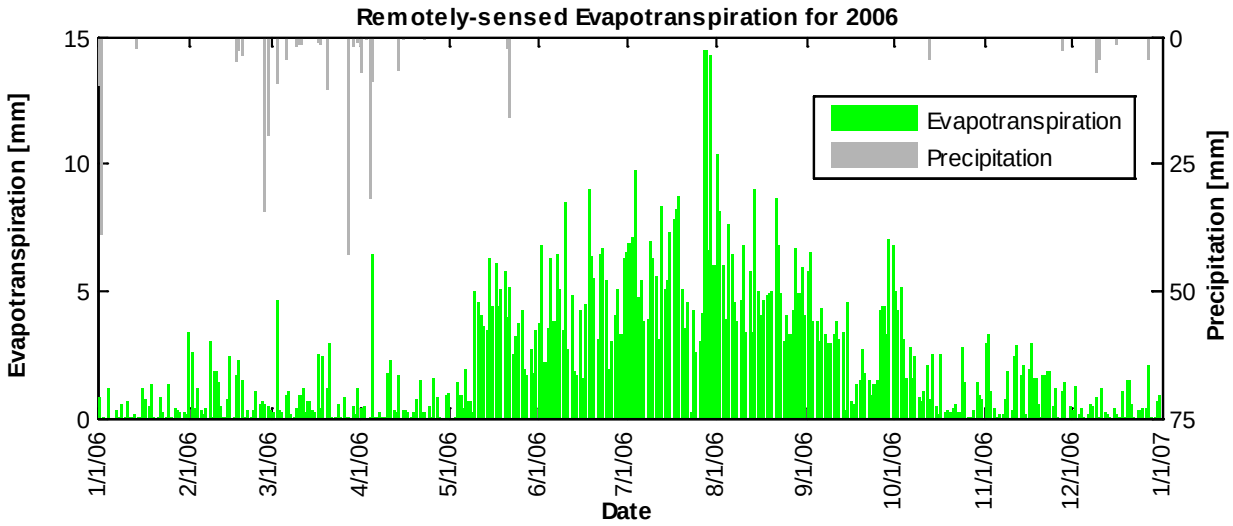

Figure 12: Remotely-Sensed Evapotranspiration for 2006 using a UCLA-Derived Algorithm

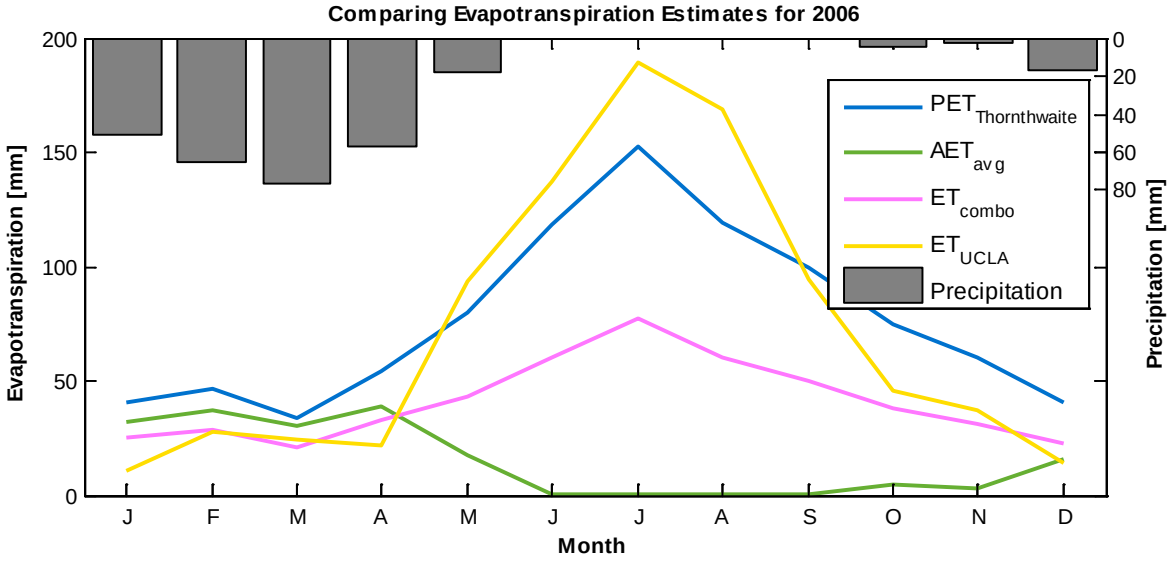

Figure 13: Comparison of Monthly Evapotranspiration Estimates during 2006

Spatial patterns of winter and summer season ET losses were compared in Figure 14 (note the difference in scale). Even though the winter snapshot was taken the day after a multi-day storm with 48 mm of P, there was not as much evaporative loss as during the summer snapshot which is after an extended dry period. Evapotranspiration during the winter was concentrated in the upper (natural) reaches of the watershed (natural areas in the Santa Monica Mountains) while during the summer it was concentrated in low density residential and rural residential land covers where irrigation was high during the dry summer months.

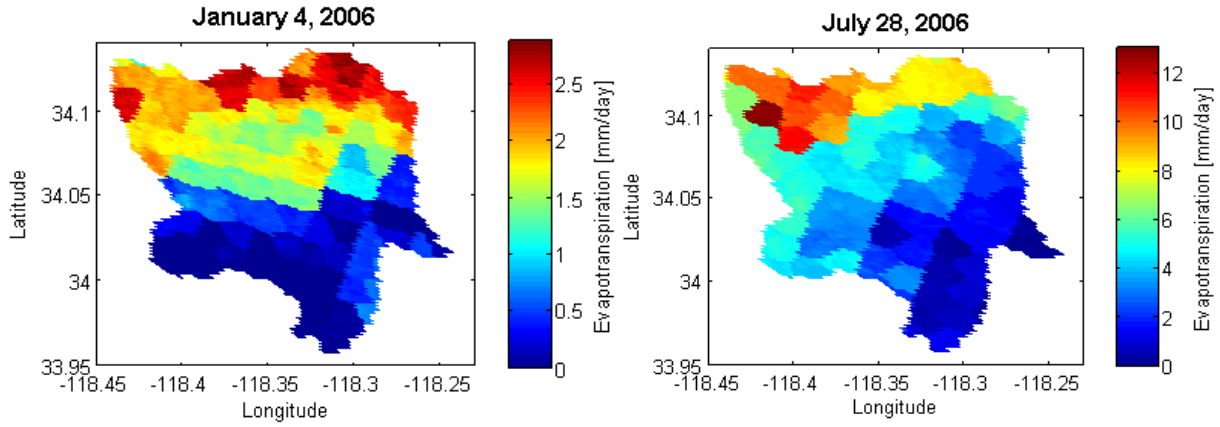

Figure 14: Winter (left) and Summer (right) Spatial Evapotranspiration Estimates for WY2006

Water Balance Results

Post-Development Water Balance

The annual water balance compares aggregated values for all four estimated components and results in the sum of Re and ε (Figure 15). The gray line represents Re and the aggregated uncertainty associated with each component. In general, the residual term (Re+ε) fluctuates based on the P pattern. Large values were observed during very wet years and near zero residual values were observed during the dry years. This pattern changed after the late 1990s where there appears to be a net decreasing trend in ε. The change in ε is still under investigation, but we hypothesize the decrease is due to increasing dry periods in the early 2000s and city-wide water restrictions, resulting in less irrigation excess R. Water balance values for each component are in Appendix C.

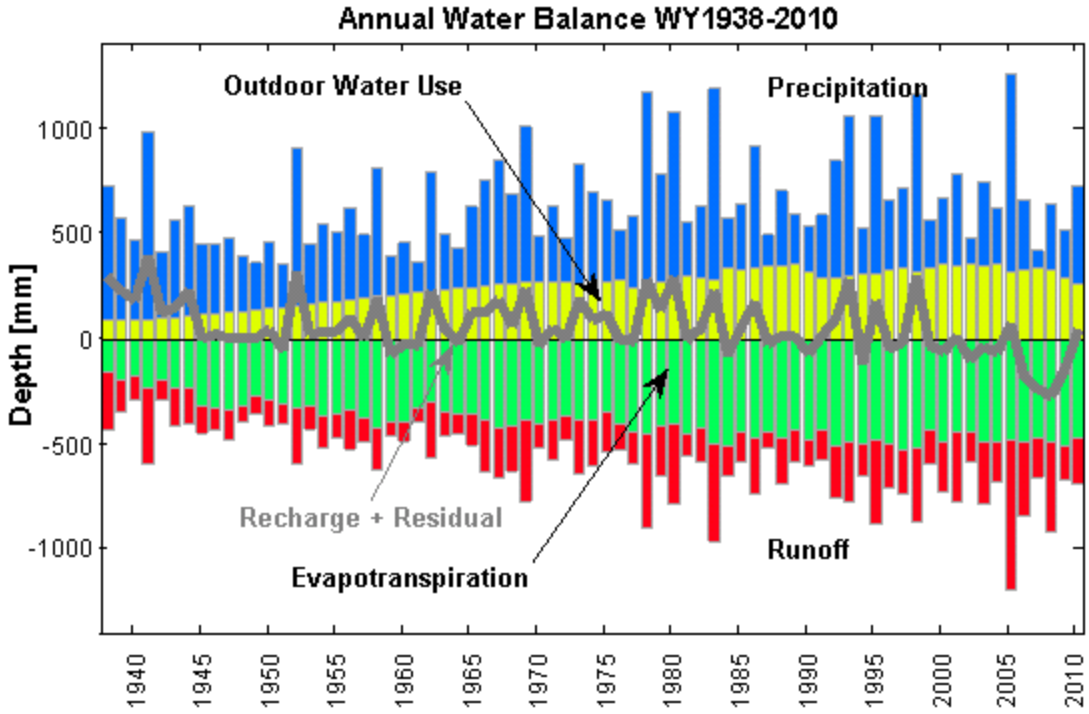

Figure 15: Post-Development Water Balance for WY1938-2010 showing outdoor water use (yellow), precipitation (blue), evapotranspiration (green), runoff (red), and recharge plus residuals (grey line).

Figure 16 shows the long-term annual average of each water balance component. Precipitation and IW combined to contribute 655 mm of input. Evapotranspiration (combo method) and R combined to produce 597 mm of output. This left the residual term to be +58 mm, which includes our model uncertainty and Re. A key component that will help to refine our water budget estimates are regional ground-water table values, and we plan to explore this in future work. In a study performed by the Los Angeles and San Gabriel Rivers Watershed Council (2010) using the Groundwater Augmentation Model (GWAM), the authors found that the percentage of P that contributes to infiltration was 25.10%, with 12.48% contributing to deep percolation (Re) in the Ballona Creek watershed. The purpose of GWAM is to model the impact of stormwater capture and infiltration to improve Re practices in Los Angeles. The GWAM models infiltration assuming that it is the amount of water remaining after interception, evaporation, and R losses immediately after P are accounted. It also models deep percolation as the change to the soil moisture due to the net effect of infiltration, irrigation, and ET. Using the GWAM estimates for recharge, the percentage of water to deep percolation during the 2000s was 43 mm (Table 3). Using this value, our model residual increases to -129 mm after removing the loss to Re from our water balance.

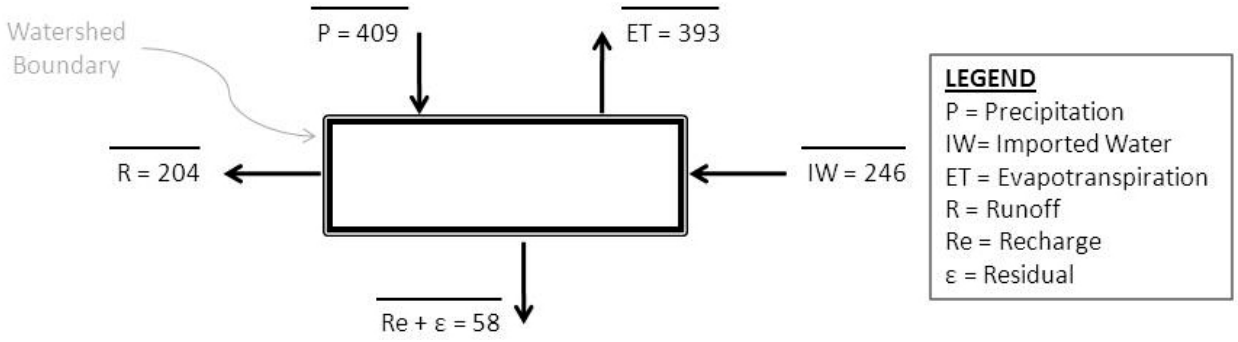

Figure 16: Long-Term Annual Post-Pevelopment Water Balance using ET_{combo} (mm) (Arrows indicate direction of watershed forcings relative to the watershed boundary; overbars indicat long-term average of water balance components)

Decadal average water balances indicate that there is a decreasing trend in the water balance residual from positive values to negative values, with the transition occurring in the most recent decade (Table 4). This may be due to the decrease in OWU due to restrictions implemented by LADWP that limit the amount of OWU, which may subsequently results in overestimates.

Table 4: Decade Annual Averages of Key Water Balance Components (mm)

Period/Decade	P	OWU	R	ET_{combo}	Re	ε
Pre-Development†	409	0	29	164	*	+216
1940s	408	117	145	267	*	+113
1950s	379	181	144	346	*	+70
1960s	406	247	187	359	*	+107
1970s	418	267	205	385	*	+95
1980s	417	322	211	436	*	+92
1990s	459	314	228	462	*	+83
2000s	343	326	302	453	*	-86
2000s‡	343	326	302	453	43	-129

Note: P is precipitation, OWU is outdoor water use, R is runoff, ET_{combo} is the combination evapotranspiration method, Re is recharge, and ε is residual.
† Based on calculations from Table 2.
* Insufficient data for infiltration estimates.
‡ Accounts for the deep groundwater recharge loss based on the GWAM model. (LASGRWC, 2010)

Pre-Development Water Balance

The pre-development water balance was calculated based on values from Table 2. The hypothesized pre-development water balance excluded the IW component (Figure 17). Precipitation was assumed to be unaffected by urbanization, so the long-term average of 409 mm was used and an R of 29 mm was utilized (Table 2). The long-term average AET_{avg} (164 mm) was used because it modeled pre-development conditions when plant growth was limited by the amount of P. The pre-development water balance residual term (Re + ε) was +216 mm, indicating a large net outward flux of water (likely towards Re). Precipitation in the mountains was not conducive to ponding, so what did not infiltrate quickly turned into overland flow. The elevation gradient in steep upper reaches provided the potential energy for R to accumulate through rill and gully flow to get to the main channel (Dingman, 2002); however, much of the R was probably lost to infiltration while en route to the main channel thus contributing to a larger groundwater outflux.

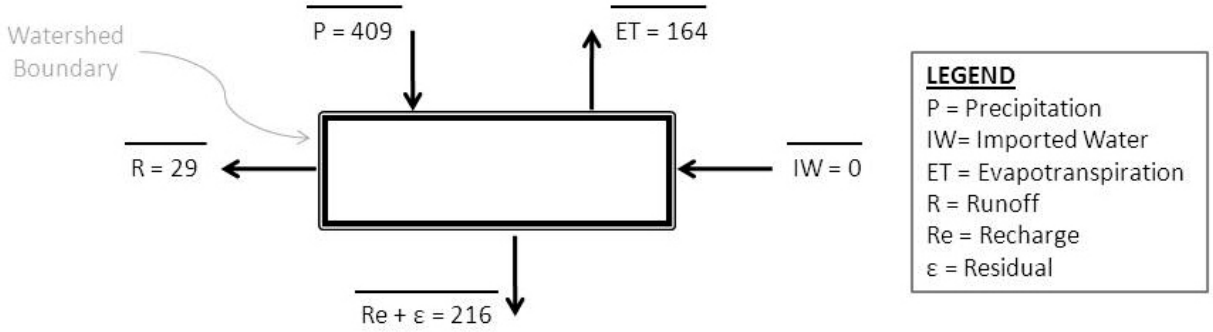

Figure 17: Hypothesized Pre-Development Water Balance (mm)

Water Balance Analysis

The water balance results provide insight on aspects of urban hydrology not well understood, including dry season partitioning of runoff, long-term water balance component variability, and sources of uncertainty. Study results impart some knowledge on these topics; though, more work is necessary to improve understanding.

Dry Season Partitioning between Native and Non-Native Water Sources

Investigation of dry season runoff and regional springs was used to partition native and non-native source contributions. Initial results indicate that 2% of July 2011 R was from native sources, while the remaining 98% was from non-native sources. July 2011 was preceded by several dry months, so there was a lengthy lag time between the P event and spring daylighting. Even though native water sources only accounted for 2%, it was quite substantial because the

spring water only came from 20% of the watershed area. The dry season spring flow contribution to runoff essentially represented its annual contribution to baseflow. Assuming dry season spring flow represents annual spring flow; springs only contributed 0.5% to the total annual runoff in WY2011. This appeared to be a negligible amount; however, this does not take into account the impact of P on spring flows. Hence, our estimates are relatively conservative; we only have dry season estimates, and we have only sampled a subset of potential springs in the watershed. Future wet season springs sampling will provide more information on the lag time between P event and daylighting flow rates. Higher springs rates are expected several days following an intense storm event. Such information would improve the estimated annual partition between native and non-native water sources.

Trends

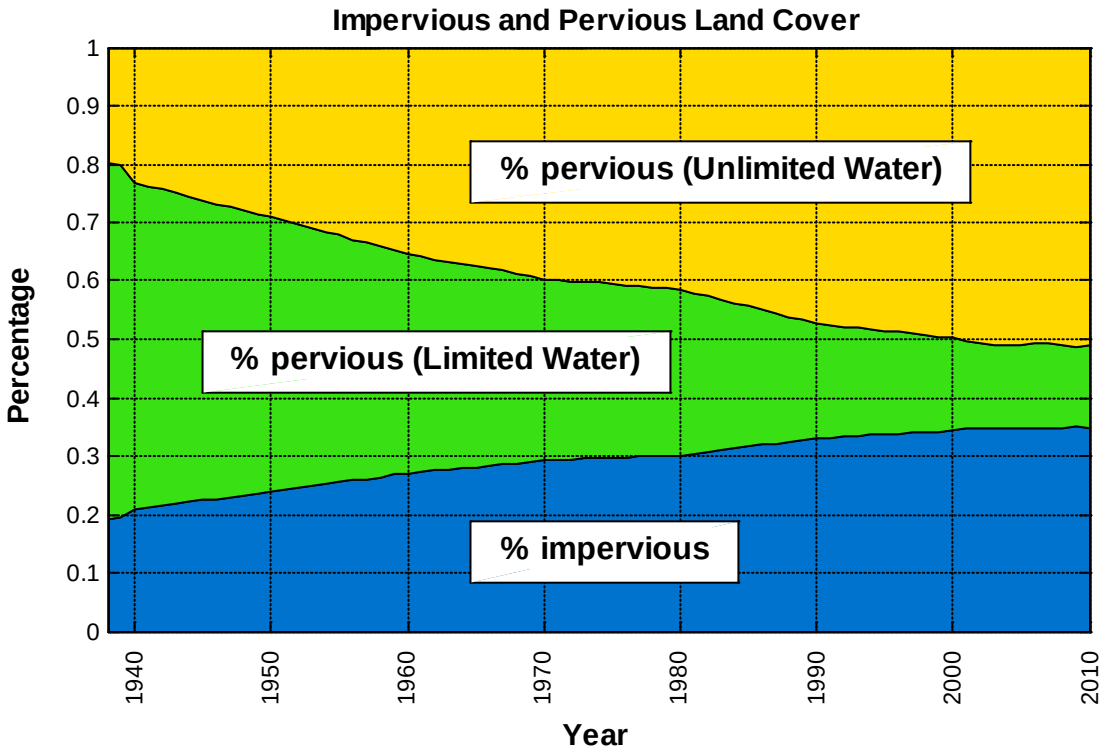

Figure 18: Trends in Total Watershed Area Divided into Impervious and Pervious Land Cover for WY1938-2010

Urbanization brought significant changes to the ground surface in the Ballona Creek watershed by replacing natural land covers, such as chaparral and sage, with developed land cover and non-native plant species. The land cover transition significantly altered surface water interactions. These interactions were partitioned into three different kinds of land cover: impervious, pervious with limited water, and pervious with unlimited water as previously discussed in the evapotranspiration section (Figure 18). Both the upward trending impervious

and pervious with unlimited water areas were direct causes for the increase in R and ET, respectively; thus raising the net amount of water cycling through the watershed. The amount of impervious area appeared to plateau in the early 2000s which may be an indication of development saturation. These land uses changes affected each water balance component to a different degree. Most components experienced an increasing trend, except P which remained consistent. Outdoor water use significantly grew with the population growth and demand over the study period. Imported water applied to outdoor uses and the increase in impervious land cover led to an increase in R year-round. Landscape irrigation allowed for near maximum levels of ET.

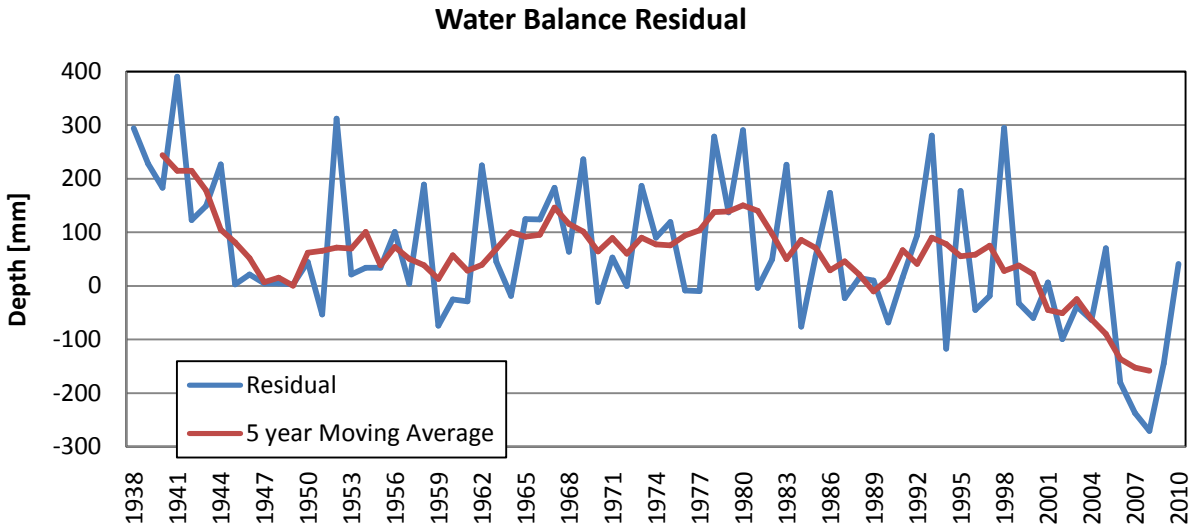

Figure 19: Trends in the Annual Water Balance Residual for the Study Period

Figure 19 shows the annual net residual of the water balance and a 5-year moving average. The 5-year moving average shows a distinct decreasing trend, which implies that Re decreased to the point where more water was entering the surface budget than leaving in the early 2000s. This trend may be attributed to large uncertainties in IW and ET estimates, as well as a lack of recharge estimates. In the last decade, the negative εmay also be the result of water use restrictions which may have reduced OWU (input), subsequently shifting ε downward.

Uncertainty in Urban Water Balance

The main categorical sources of uncertainty was physical sources, which include unaccounted springs in the runoff partitioning, inaccurate partitioning of indoor water use and OWU, poor ET estimates, poor quality pressure transducer data, inability of rating curves to provide accurate estimations, linearity between impervious area and population, simplified data aggregation methods, and inability to separate recharge from ε to determine the true water balance residual. Because it was impossible to find all springs, whether intermittent or perennial,

the number of springs directly affected runoff partitioning. Residential water use partitioning was based on published values and weighted based on the land cover in the watershed, but this assumed that the published values were accurate for Ballona. Similarly, the impact of impervious land cover combined with irrigated land cover made ET estimation a challenge. In the end, the net residual of urban water balances resulted in deep groundwater movement and residual error, but it was difficult to separate the two and determine the amount of uncertainty. Other sources of error included human measurement error, gauge malfunction, missing data, and data quality errors. Flows that could not be measured using an electronic meter, required rudimentary methods, such as the float method and bag test, which affected flow estimates used in rating curve development and runoff partitioning. Gauge malfunction was unpredictable and affected data continuity, particularly for the sub-watershed runoff estimates. Missing data was filled using linear relationships; however, not all of these variables actually behaved linearly, which introduced sources of error to the estimations.

Data quality early during the study period was likely not as good as contemporary data. Back-scaling data using the linear correlation between annual values possibly amplified error propagation in historical estimates. We hypothesize that the contemporary post-development water balance underestimates both ET and OWU, and that the %OU also may be biased low. LADWP estimates landscape water use to be 40 to 70% of total residential water use. Although there are many uncertainties with the urban water balances, minimizing the uncertainties may be possible with improved methods. Considering the various hydrologic components used in this study and published estimates of uncertainty, we estimate our final annual water balance residual to have an uncertainty of ~40%. We base this value on published values of uncertainty in P (5 - 10%) and streamflow observations (5 - 15%; Winter, 1981), and our estimate of evaporation estimate uncertainty (25%). We also note significant uncertainty in the estimate of native water in the system based on our springs measurements, likely up to 100%.

Summary and Future Work

In the current study, we were able to estimate each of the water balance components and reduce the residual term to about 9% of the long-term input. However, additional work is needed to further reduce this residual term. Improved estimates of ET, native and non-native source partitioning of R, OWU, and groundwater table fluctuations will reduce our overall uncertainties. In particular, remotely-sensed ET estimates from 2000 to 2010 will improve the contemporary water budget and help guide our historical ET estimates. Sampling of the known springs throughout the year will improve our understanding of the lag time between P and daylighting of natural springs, particularly during the wet season. Improved OWU estimates through the Urban Long Term Research Areas (ULTRA) in Los Angeles will also minimize estimation errors. Integration of groundwater table values will help to verify the change in the system due to recharge. Lastly, a sensitivity analysis on model parameters will quantify areas with significant uncertainty in our conceptual watershed model.

Acknowledgements

We would like to acknowledge the assistance of Dr. Jongyoun Kim on the remote sensing work for this project and the numerous students who assisted with the data collection and field sampling throughout this project, including: Kristine Gali, Savoth Hy, Zhao Yang, Chris Wessel, Sara Miller, Forest Pfeiffer, Eric Hennesbaugh, David Moering, Brandon Hale, Jeff Roubos, Carolyn Chou, and Paige Russell. Funding for this project was provided by the Santa Monica Bay Restoration Commission.

References

Bhaduri B., J. Harbor, B. Engel, and M. Grove. (2000) “Assessing Watershed-Scale, Long-Term Hydrologic Impacts of Land-Use Change Using a GIS-NPS Model.” *Environmental Management* 26.6,643–658.

Blaney, H.F. and W.D. Criddle. (1962) "Determining consumptive use and irrigation water requirements.” U. S. Dept. Agriculture. Agricultural Research Service Tech Bulletin 1275, 59.

Braa, B., J. Hall, C-C. Lian, and G. McCollum. (2001) *Seeking Springs: A landscape framework for urban and ecological revitalization in the upper Ballona Creek watershed.*

Budyko, M. I. (1974) Climate and Life. Academic Press, New York, NY.

Chauvin, G.M., G.N. Flerchinger, T.E. Link, D. Marks, A.H. Winstral, and M.S. Seyfried. (2011) "Long-term water balance and conceptual model of a semi-arid mountainous catchment." *Journal of Hydrology.* 400, 133-143.

Dark, S., E.D. Stein, D. Bram, J. Oscuna, J. Monteferante, T.Longcore, R. Grossinger,and E. Beller (2011) “Historical Ecology of the Ballona Creek Watershed.” Southern California Coastal Water Research Project Technical Report #671.

Chow, V.T. (1959) *Open-channel Hydraulics.* McGraw- Hill Book Co., New York.

Dingman, S.L. (2002) *Physical Hydrology*. Macmillan College Publishing Co., New York, 575.

Garcia-Fresca, B. (2005) “Urban-enhanced groundwater rechargeL review and case study of Austin, Texas, USA. Draft Report, University of Texas at Austin.

Gleick, P., D. Haasz, C. Henges-Jeck, V. Srinivasan, G. Wolff, K.K. Cushing, and A. Mann. (2003) Waste not, want not: the potential for urban water conservation in California. Pacific Institute.

Hall, W.H. (1888) "Irrigation in California [Southern]- Part II" J.D. Young, Supt. State Printing.

Hargreaves, G.H. (1947) *A Suggested Method of Standardizing Irrigation Requirements for the Central Valley (Calif.) Crops*. U.S. department of the Interior, Bureau of Reclamation. Boise, ID.

He, M. and T.S. Hogue. (2011) "Integrating hydrologic modeling and land use projections for evaluation of hydrologic response and regional water supply impacts in semi-arid environments." *Environmental Earth Sciences*, DOI 10.1007/s12665-011-1144-3.

Heberger, M., H. Cooley, P. Herrera, P.H. Gleick, and E. Moore (2009) “The impacts of sea-level rise on the California coast”. Pacific Institute Technical Report CEC-500-2009-024-F

Hogue, T.S. (2009) "Predicting the Impacts of Urbanization on Basin-scale Runoff and Infiltration in Semi-arid Regions" University of California Water Resources Center Technical Completion Report WR 1007.

Joint Institute for the Study of the Atmosphere and Ocean. Pacific Decadal Oscillation and Global-SST ENSO Climate Indices. University of Washington. Web. <http://jisao.washington.edu/data/> 18 July 2011.

Kim, J. and T.S. Hogue (2008). “Evaluation of a MODIS-Based Potential Evapotranspiration Product at the Point Scale.” *Journal of Hydrometerology* 7 (2008):444-460.

Los Angeles and San Gabriel Rivers Watershed Council (LASGWC). (2010) Water Augmentation Study- Research, Strategy, and Implementation Report. LASGWC. Alhambra, CA.

Los Angeles County Department of Public Works Spatial Information Library. ArcGIS shapefiles and geodatabases. < http://gis.dpw.lacounty.gov/oia/> May 2010.

Los Angeles County Department of Public Works, Ballona Creek Renaissance, Los Angeles City Department of Public Works (Bureau of Sanitation, Watershed Protection Division), National Park Service, and Santa Monica Bay Restoration Commission. (2004) Ballona Creek Watershed Management Plan (BCWMP).

Los Angeles County Department of Public Works (LACDPW). (2006) Los Angeles County Hydrology Manual. LACDPW,.Alhambra, CA.

Los Angeles Department of Water and Power. (2010) Urban Watershed Management Plan. LADWP. Los Angeles, CA

Mays, L.W. (2005). *Water Resources Engineering.* Wiley. Hoboken, NJ.

McKee, T.B., N.J. Doesken, and J. Kleist. (1993) Standardized Precipitation Index. Colorado State University. Web. <http://drought.unl.edu/> 06 July 2011.

Nash, L.L. and P.H. Gleick. (1991) "Sensitivity of streamflow in the Colorado basin to climatic changes." *Journal of Hydrology* 125, 221-241.

Ol’dekop, E. M. (1911) “On evaporation from the surface of river basins” (in Russian). Transactions on Meteorological Observations, University of Tartu Review 4, 200.

Schreiber, P. U. (1904) “ber die Beziehungen zwischen dem Niederschlag und der Wasserfu¨ hrung der Flu¨ sse in Mitteleuropa.” *Meteorolgique Z* 21, 441–452.

Thornthwaite, C.W. (1948) “An approach toward a rational classification of climate” *Geographical Review* 38, 55–94.

Turc, L. (1954) “Le bilan d’eau des sols. Relation entre la pre´ -cipitation, l’e´ vaporation et l’e´coulement.” *Annales Agronomiques* 5, 491–569.

United States Geological Survey. (1992) *1992 National Landcover Database*. USGS. Reston, VA.

Weng, Q. (2001) “Modeling Urban Growth Effects on Surface Runoff with the Integration of Remote Sensing and GIS.” *Environmental Management* 28.6, 737-748.

Winter, T.C. (1981). Uncertainties in estimating the water balance of lakes. *Water Resources Bulletin* 17, 82-115.

Appendix A - Data Sources

Table A - 1: Precipitation Gauge Information

Source	ID	Gauge Name	Period of Record		Gage Datum (feet above sea level)
			Start WY	End WY	
LAC DPW	310	LA City College	2002	2008	300
	312	Hollywood Reservoir	1993	2010	720
	316	LA 96th	1996	2010	121
	322	Sepulveda Canyon	1997	2010	1425
	323	Bel Air Hotel	1997	2009	540
	370	Ballona Creek @ Sawtelle	1995	2010	38
	375	USC	2006	2010	208
	377	LA Ducommun Street	1997	2010	306
	403	Hillcrest Country Club	2005	2010	185
NCDC	049152	UCLA	1938	2010	430
	045115	Los Angeles WBO	1922	2010	312
	040619	Bel Air FC 10a	1949	1980	541
	045111	LA 6th and Main	1949	1951	410
	045112	LA Terminal A	1949	1953	279

Note: LACDPW is Los Angeles County Department of Public Works, NCDC is National Climactic Data Center

Table A - 2: Air Temperature Gauges

Source	ID	Gauge Name	Period of Record		Gage Datum (feet above sea level)
			Start WY	End WY	
NCDC	042214	Culver City	1936	2010	55
	045115	Downtown USC/ Los Angeles WBO	1922	2010	312
	046256	North Hollywood	1938	1960	620
	049152	UCLA	1934	2010	430
CDEC	BHL	Beverly Hills	2005	2009	1260

Note: NCDC is National Climactic Data Center, CDEC is California Data Exchange Center (Department of Water Resources

Table A - 3: CIMIS Gauge Information

Source	ID	Gauge Name	Period of Record		Gage Datum (feet above sea level)
			Start WY	End WY	
CIMIS	99	Santa Monica	1993	2010	340

Table A - 4: MODIS Satellite Data for Evapotranspiration Estimates

Short Name	Full Name
MCD43B3	MODIS/Terra+Aqua Albedo 16-Day L3 Global 1km SIN Grid V005
MOD03	MODIS/Terra Geolocation Fields 5-Min L1A Swath 1km V005
MOD04_L2	MODIS/Terra Aerosol 5-Min L2 Swath 10km V005
MOD05_L2	MODIS/Terra Total Precipitable Water Vapor 5-Min L2 Swath 1km and 5km V005
MOD06_L2	MODIS/Terra Clouds 5-Min L2 Swath 1km and 5km V005
MOD07_L2	MODIS/Terra Temperature and Water Vapor Profiles 5-Min L2 Swath 5km V005
MOD11_L2	MODIS/Terra Land Surface Temperature/Emissivity 5-Min L2 Swath 1km V005
MOD13Q1	MODIS/Terra Vegetation Indices 16-Day L3 Global 250m SIN Grid V005
MYD13Q1	MODIS/Aqua Vegetation Indices 16-Day L3 Global 250m SIN Grid V005

Table A - 5: Runoff Gauge Information

Source	ID	Gauge Name	Period of Record		Gage Datum (feet above sea level)
			Start WY	End WY	
LAC DPW	F38C	Ballona Creek	1931	2010	12

Table A - 6: Sub-watershed Flow Field Log

Date	Tasks Completed
11/12/2009	• HOBOs and HOBO housings were installed. • HOBOs were setup for the initial data collection.
11/24/2010	• HOBOs were checked to see if they were functioning properly • Downloaded HOBO data, cleared HOBO, and recommenced the HOBO data collection.
1/7/2010	• Downloaded HOBO data, cleared HOBO, and recommenced the HOBO data collection.
2/28/2010	
4/17/2010	
5/22/2010	
7/16/2010	
9/24/2010	
11/12/2010	
1/7/2011	
3/2/2011	• All HOBOs were removed • Downloaded HOBO data, cleared HOBO, and recommenced the HOBO data collection

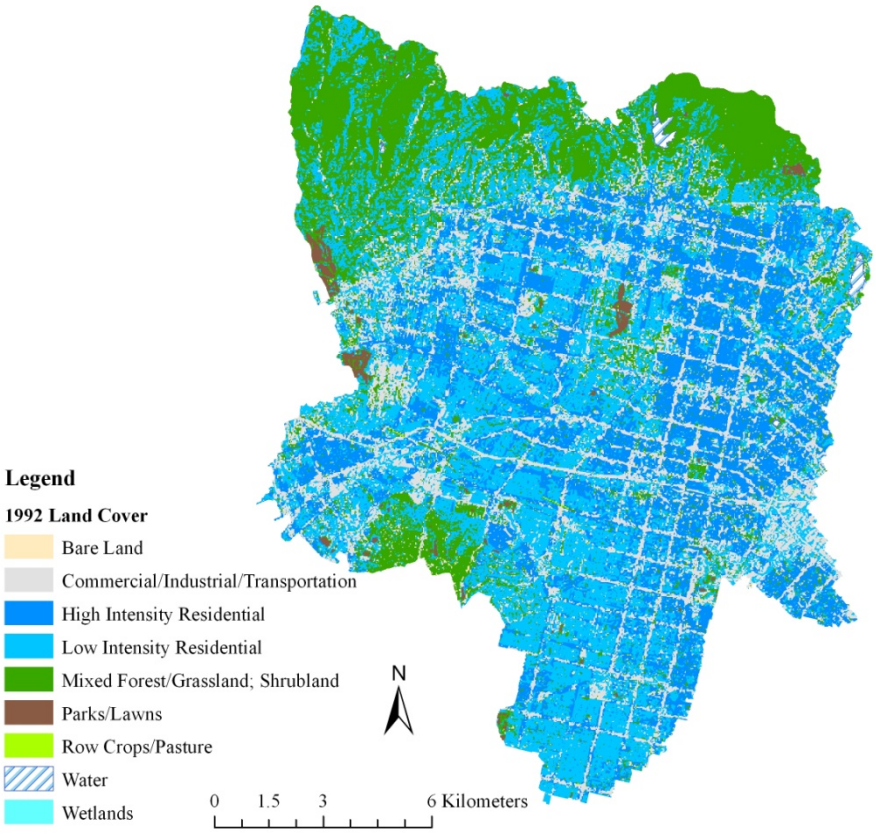

Figure A - 1: 1992 Land Cover Map (USGS National Landcover Database, 1992)

Table A - 7: 1992 Land Cover Breakdown by Area

Type	**Area [km^2]**	**% Area**
Bare Land	1.77	0.8%
Commercial/Industrial/Transportation	62.55	27.1%
High Intensity Residential	42.52	18.4%
Low Intensity Residential	88.19	38.2%
Mixed Forest/Grasslands	32.15	13.9%
Parks/Lawns	3.03	1.3%
Row Crops/Pasture	0.19	0.1%
Water	0.13	0.1%
Wetlands	0.05	0.0%

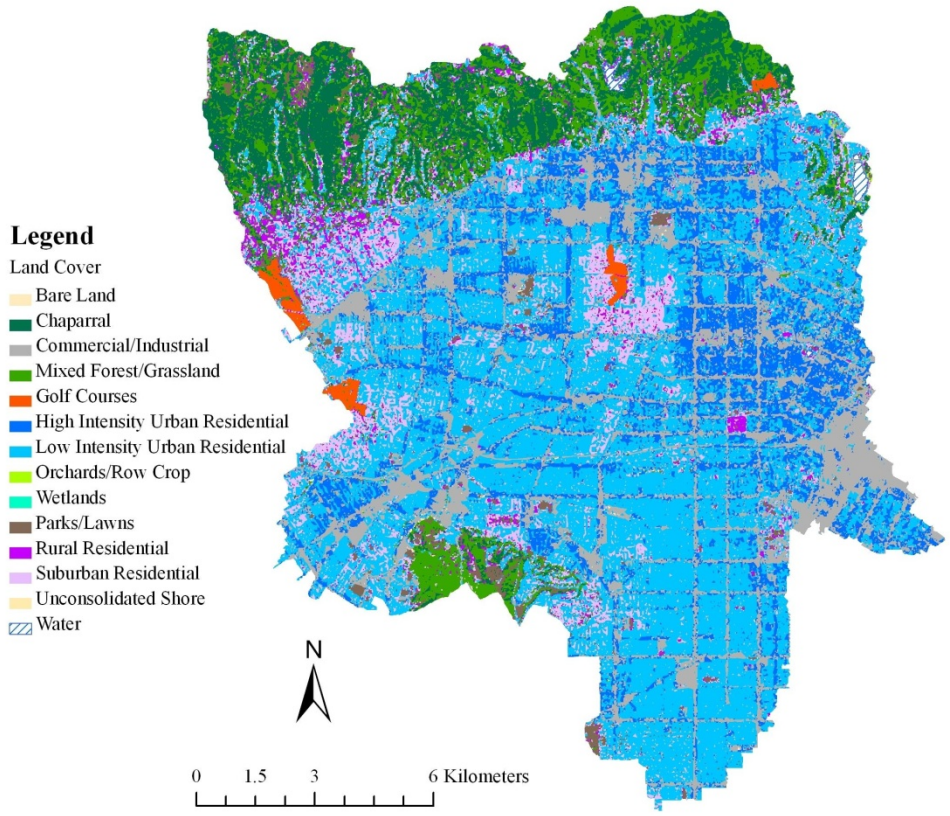

Figure A - 2: 2001 Land Cover (NOAA Coastal Change Analysis Project (C-CAP))

Table A - 8: 2001 Land Cover Breakdown by Area

Type	**Area [km^2]**	**% Area**
Bare Land	0.18	0.1%
Chaparral	22.99	10.0%
Commecial/Industrial	36.25	15.7%
Mixed Forest/Grassland	18.72	8.1%
Golf Course	1.82	0.8%
High Intensity Urban Residential	30.65	13.3%
Low Intensity Urban Residential	86.52	37.5%
Orchards/Row Crop	0.10	0.0%
Wetlands	0.14	0.1%
Parks/Lawns	4.48	1.9%
Rural Residential	6.08	2.6%
Suburban Residential	22.09	9.6%
Unconsolidated Shore	0.03	0.0%
Water	0.55	0.2%

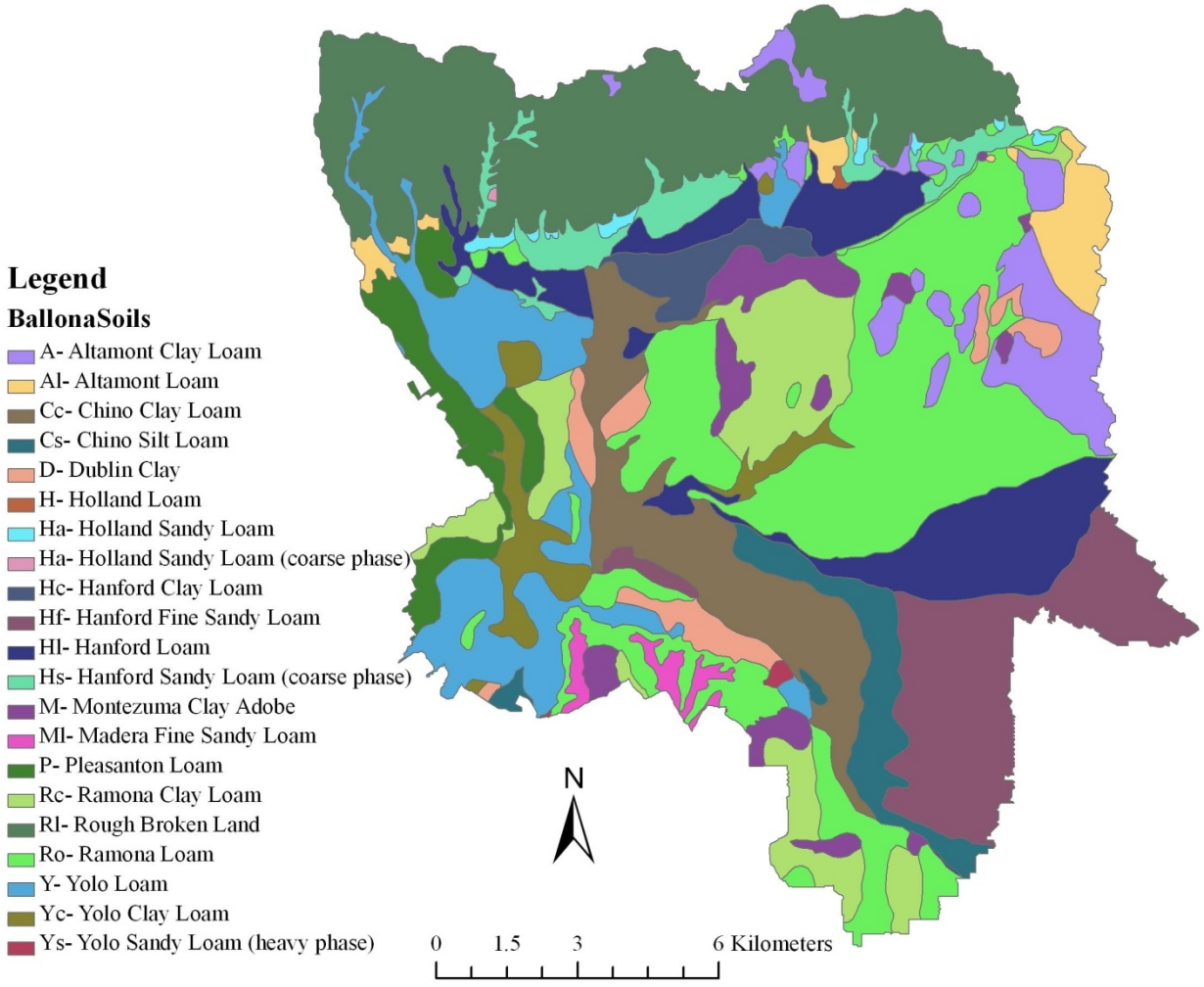

Figure A - 3: 1916 Soil Survey- Los Angeles Sheet (Nelson et al., 1916)

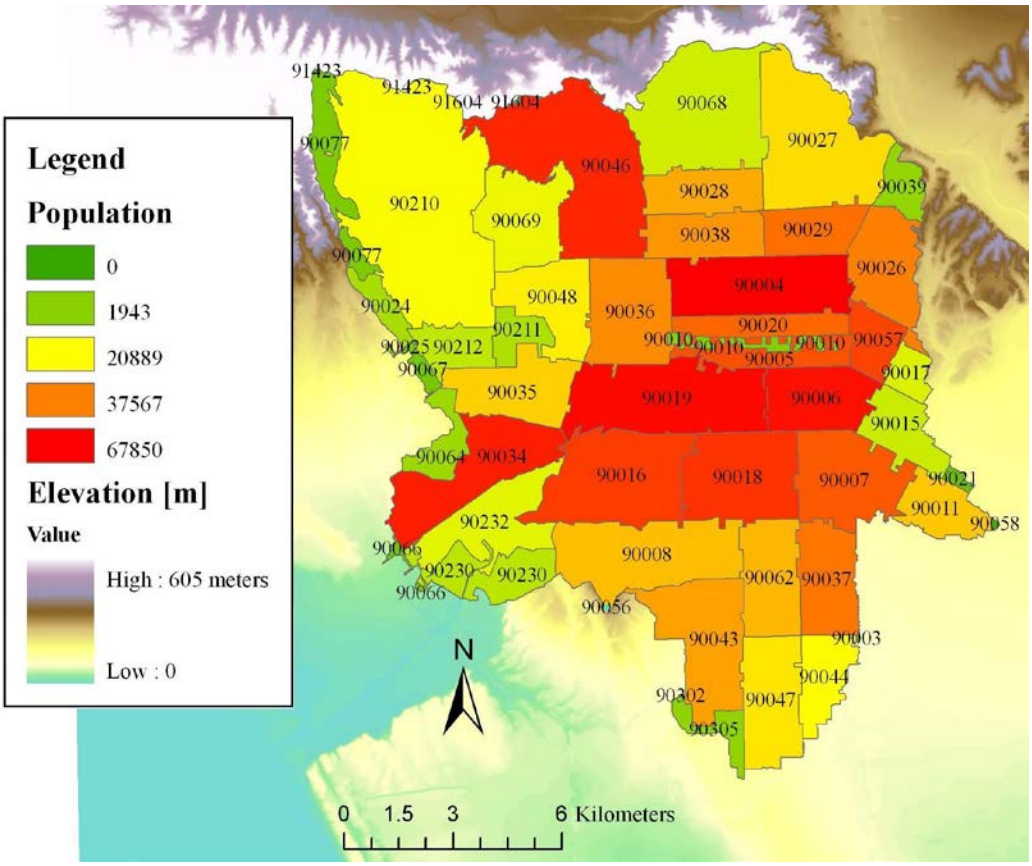

Figure A - 4: 2000 Population by Zip Code (U.S. Census Bureau, 2000)

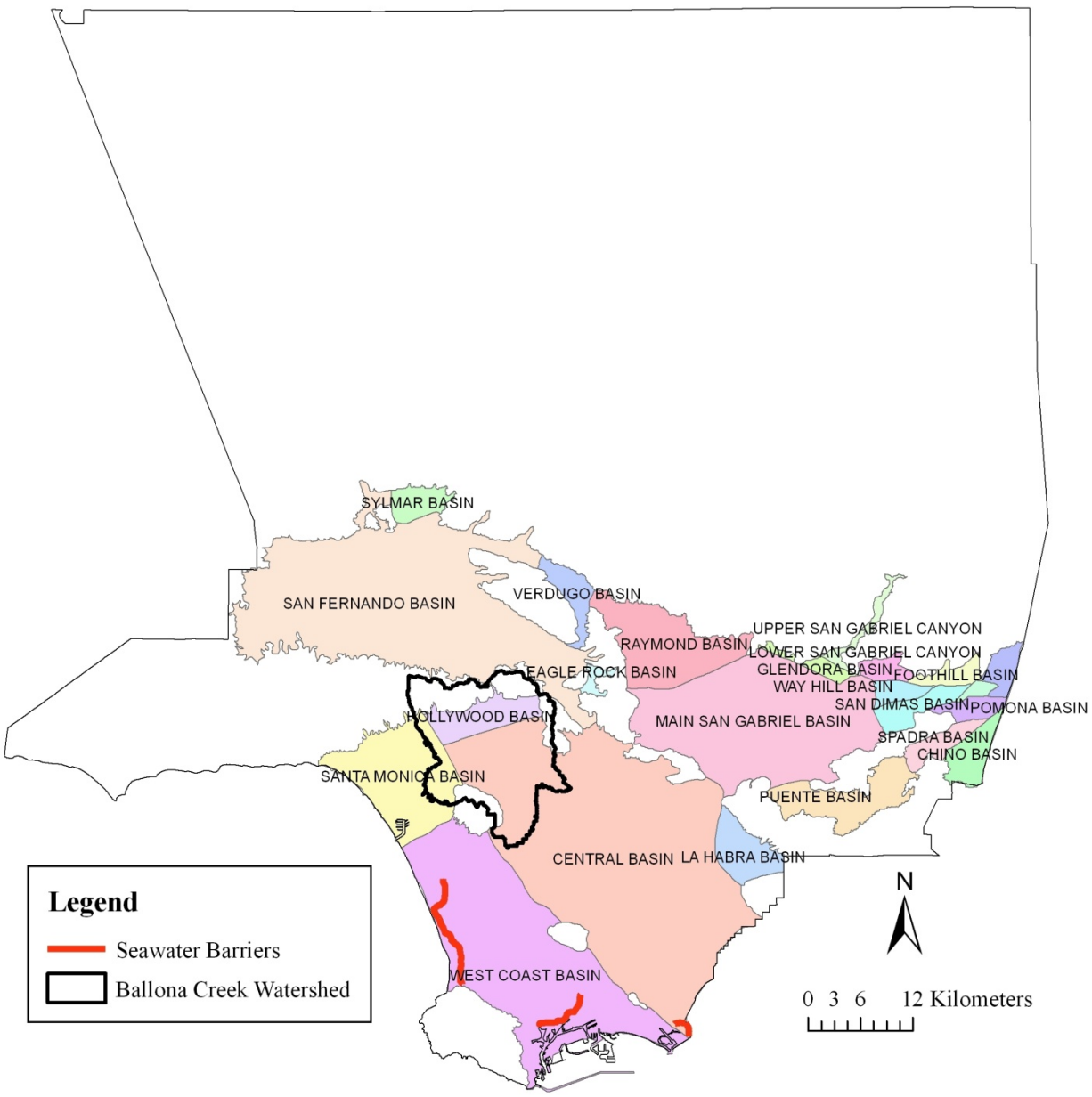

Figure A - 5: Groundwater Basins in Los Angeles County Near Ballona Creek

Appendix B - Methods

Thiessen Polygon Method

The Thiessen Polygon method was used to assign an area of influence to each gauge based on its relative location. Perpendicular bisectors were drawn and extended to create polygons. After overlaying the watershed boundary, the area of influence for each gauge was determined. The percentage of each of these areas to the total watershed area produced the areal weights. This method was used to calculate both mean areal precipitation and evapotranspiration (see below).

$$MAP = \sum_{n=1}^{N} P_n \times \left(\frac{A_n}{A_T} \right)$$ **Equation B - 1**

Where:

MAP is mean areal precipitation (or the basin average), P_n is the precipitation for gauge N, A_n is the area of polygon around gauge N, A_T is total area of watershed, and N is the number of gauges.

Table B - 1: Hypothesized Relative Change (♦) to Each Water Balance Component

ID	Variable	Pre-Development	Post-Development	
			Early	Late
P	Precipitation	♦	♦	♦
ET	Evapotranspiration	♦	♦♦	♦♦♦
R	Runoff	♦	♦♦	♦♦♦
IW	Imported Water	None	♦♦	♦♦♦
I/Re	Infiltration/Recharge	♦♦♦	♦♦	♦
Re	Groundwater Recharge	♦♦	♦	♦
	Natural Springs	♦♦♦	♦♦	♦
	Pumping	Minimal	♦	♦
ε	Residual	???	???	???

For sub-watershed flows, measured water depths were first calculated using the temperature and pressure data, then corresponding flow rates were read off of their respective rating curves.

REFERENCE EVAPOTRANSPIRATION (ETO) EQUATIONS

Blaney-Criddle Method (Blaney and Criddle, 1962)

$$ET_o(cm/month) = (0.142T_a - 1.095)(T_a + 17.8) \times K \times d \qquad \textbf{Equation B - 2}$$

T_a = average air temperature (^{o}C)

K = empirical crop factor accounting for crop type and growth stage

d = the fraction of annual hours of daylight for the month

Table B - 2: Monthly fraction of annual hours of daylight (d)

Latitude	Jan	Feb	Mar	Apr	May	Jun	Jul	Aug	Sep	Oct	Nov	Dec
60	0.047	0.057	0.081	0.096	0.117	0.124	0.123	0.107	0.086	0.070	0.050	0.042
50	0.060	0.063	0.082	0.092	0.107	0.109	0.110	0.100	0.085	0.075	0.061	0.056
40	0.067	0.066	0.082	0.089	0.099	0.100	0.101	0.094	0.083	0.077	0.067	0.075
20	0.073	0.070	0.084	0.087	0.095	0.095	0.097	0.092	0.083	0.080	0.072	0.072
10	0.081	0.075	0.085	0.084	0.088	0.086	0.089	0.087	0.082	0.083	0.079	0.081
0	0.085	0.077	0.085	0.082	0.085	0.082	0.085	0.085	0.082	0.085	0.082	0.085
-10	0.089	0.079	0.085	0.081	0.082	0.079	0.081	0.083	0.082	0.086	0.085	0.088
-20	0.092	0.081	0.086	0.079	0.079	0.074	0.078	0.080	0.081	0.088	0.089	0.093
-30	0.097	0.083	0.086	0.077	0.074	0.070	0.073	0.078	0.081	0.090	0.092	0.099
-40	0.102	0.086	0.087	0.075	0.070	0.064	0.068	0.074	0.080	0.092	0.097	0.105

Table B - 3: Empirical crop factors (K) (from the US Soil Conservation Service)

Crop	Jan	Feb	Mar	Apr	May	Jun	Jul	Aug	Sep	Oct	Nov	Dec
Pasture grass	0.49	0.57	0.73	0.85	0.90	0.92	0.92	0.91	0.87	0.79	0.67	0.55
Alfalfa	0.63	0.73	0.86	0.99	1.08	1.13	1.13	1.06	0.99	0.91	0.78	0.64
Grapes	0.20	0.24	0.33	0.50	0.71	0.80	0.80	0.76	0.61	0.50	0.35	0.23
Deciduous orchard	0.17	0.25	0.40	0.63	0.88	0.96	0.96	0.82	0.54	0.30	0.19	0.15

Potential Evapotranspiration (PET) Equations

Hargreaves Method (Hargreaves, 1947)

$$PET(mm/day) = 0.0023 S_o (T_a + 17.8)\sqrt{\delta_T}$$ **Equation B - 3**

S_o = water equivalent of extraterrestrial solar radiation (mm day^{-1})

$$S_o(mm/day) = 15.392 d_r (\omega_s \sin\phi \sin\delta + \cos\phi \cos\delta \sin\omega_s)$$

T_a = average air temperature (°C)

δ_T = change in daily minimum and maximum air temperature (°C)

Where variables in S_o are defined as:

$$d_r = 1 + 0.033 \cos\left(\frac{2\pi}{365} J\right)$$

$$\omega_s = \arccos(-\tan\phi \tan\delta)$$

$$\delta = 0.4093 \sin\left(\frac{2\pi}{365} J - 1.405\right)$$

d_r = relative distance between the earth and the sun

ω_s = sunset hour angle (radians)

φ = latitude (+ for Northern Hemisphere, - for Southern Hemisphere)

δ = solar declination (radians)

J = Julian day

Thornthwaite Method (Thornthwaite, 1948)

$$PET(mm/month) = 16b\left(\frac{10T_a}{I}\right)^a$$ **Equation B - 4**

T = average air temperature (°C)

$$I = \sum_{l}^{12}\left(\frac{T_a}{5}\right)^{1.514}$$ (per wateryear)

a = an empirical function of I

$$a = 6.7x10^{-7}I^3 - 7.7x10^{-5}I^2 + 1.8x10^{-2}I + 0.49$$

b = monthly adjustment factor related to hours of daylight (see table)

Table B - 4: b correction factor based on latitude and month of year

Latitude	Jan	Feb	Mar	Apr	May	Jun	Jul	Aug	Sep	Oct	Nov	Dec
60	0.54	0.67	0.97	1.19	1.33	1.56	1.55	1.33	1.07	0.84	0.58	0.48
50	0.71	0.84	0.98	1.14	1.28	1.36	1.33	1.21	1.06	0.90	0.76	0.68
40	0.80	0.89	0.99	1.10	1.20	1.25	1.23	1.15	1.04	0.93	0.83	0.78
30	0.87	0.93	1.00	1.07	1.14	1.17	1.16	1.11	1.03	0.96	0.89	0.85
20	0.92	0.96	1.00	1.05	1.09	1.11	1.10	1.07	1.02	0.98	0.93	0.91
10	0.97	0.98	1.00	1.03	1.05	1.06	1.05	1.04	1.02	0.99	0.97	0.96
0	1.00	1.00	1.00	1.00	1.00	1.00	1.00	1.00	1.00	1.00	1.00	1.00
-10	1.05	1.04	1.02	0.99	0.97	0.96	0.97	0.98	1.00	1.03	1.05	1.06
-20	1.10	1.07	1.02	0.98	0.93	0.91	0.92	0.96	1.00	1.05	1.09	1.11
-30	1.16	1.11	1.03	0.96	0.89	0.85	0.87	0.93	1.00	1.07	1.14	1.17
-40	1.23	1.15	1.04	0.93	0.83	0.78	0.80	0.89	0.99	1.10	1.20	1.25
-50	1.33	1.19	1.05	0.89	0.75	0.68	0.70	0.82	0.97	1.13	1.27	1.36

Actual EVAPOTRANSPIRATION (AET) EQUATIONS

Budyko Method (Budyko, 1974)

The Budyko equation is based on a geometric mean of the Ol'dekop (1911) and Schreiber (1904) methods. $AET(mm/\ period) = P \times \sqrt{\frac{PET}{P} \times \tanh\left(\frac{P}{PET}\right) \times \left(1 - e^{-PET/P}\right)}$

Equation B - 5

Ol'dekop Method (Ol'dekop, 1911)

$$AET(mm/\ period) = PET \times \tanh\left(\frac{P}{PET}\right)$$ **Equation B - 6**

Schreiber Method (Schreiber, 1904)

$$AET(mm/\ period) = P\left(1 - e^{-PET/P}\right)$$ **Equation B - 7**

Turc Method (Turc, 1954)

$$AET(mm/\ period) = \frac{P}{\sqrt{0.9 + \left(\frac{P}{PET}\right)^2}}$$ **Equation B - 8**

Appendix C - Results

Table C - 1: Annual Water Balance parameters [mm]

WY	P	OWU	R	ET_{combo}
1938	641	86	281	151
1939	486	86	152	192
1940	384	86	113	173
1941	890	92	360	231
1942	314	97	92	196
1943	461	103	183	231
1944	523	108	176	228
1945	334	114	131	314
1946	329	120	98	330
1947	356	125	141	336
1948	263	131	73	317
1949	224	136	86	272
1950	316	142	124	289
1951	202	149	101	304
1952	746	156	262	329
1953	286	163	107	321
1954	376	170	152	361
1955	329	178	116	357
1956	437	185	185	335
1957	301	192	119	370
1958	613	199	202	421
1959	183	206	73	390
1960	245	213	92	391
1961	146	219	67	327
1962	565	225	268	298
1963	269	231	115	341
1964	197	237	96	357
1965	384	244	147	355
1966	499	250	238	387
1967	588	256	242	418
1968	427	262	217	408
1969	738	268	392	379
1970	215	274	119	400
1971	360	267	190	384
1972	207	274	121	360
1973	561	263	255	382
1974	426	267	220	383
1975	390	268	190	349
1976	236	280	123	401
1977	343	238	151	440
1978	923	247	441	450
1979	517	265	235	410
1980	798	275	380	402
1981	257	294	108	447
1982	343	287	160	421
1983	902	283	461	499
1984	239	333	145	504
1985	306	330	146	436
1986	578	333	265	473
1987	151	342	77	439
1988	361	343	223	466
1989	234	356	149	432
1990	216	319	125	478
1991	304	284	145	427
1992	556	290	242	511
1993	759	297	292	483
1994	225	304	151	496
1995	751	303	398	478
1996	330	326	207	494
1997	383	335	212	525
1998	842	315	351	512
1999	226	337	161	434
2000	315	352	238	489
2001	435	347	334	441
2002	122	359	143	438
2003	394	348	295	486
2004	265	351	189	490
2005	933	321	705	479
2006	332	326	348	491
2007	86	332	184	472
2008	313	327	428	483
2009	231	287	158	505
2010	465	263	214	473
Avg	**409**	**246**	**204**	**393**

Note: P is precipitation, OWU is outdoor water use, R is runoff, and ET_{combo} is a combination of modified actual evapotranspiration and modified potential evapotranspiration

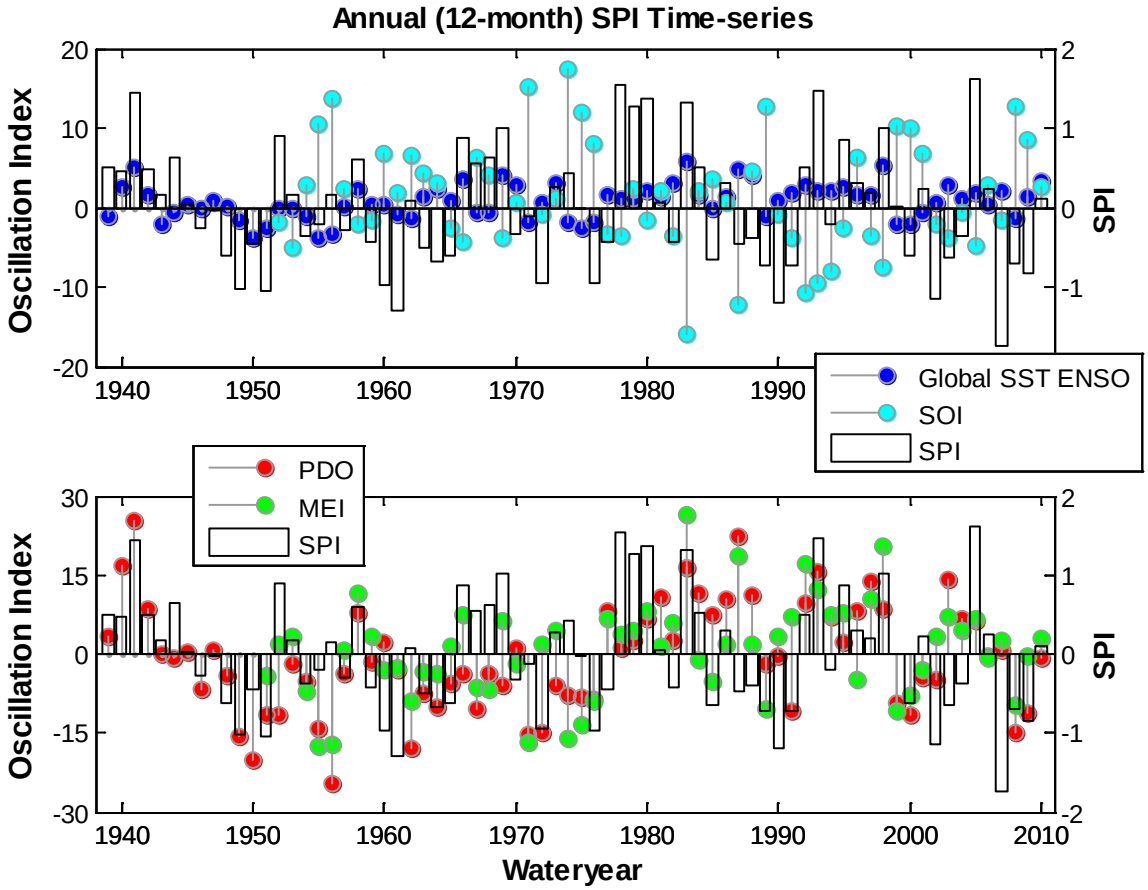

Figure C - 1: Annual SPI and Climate Indices

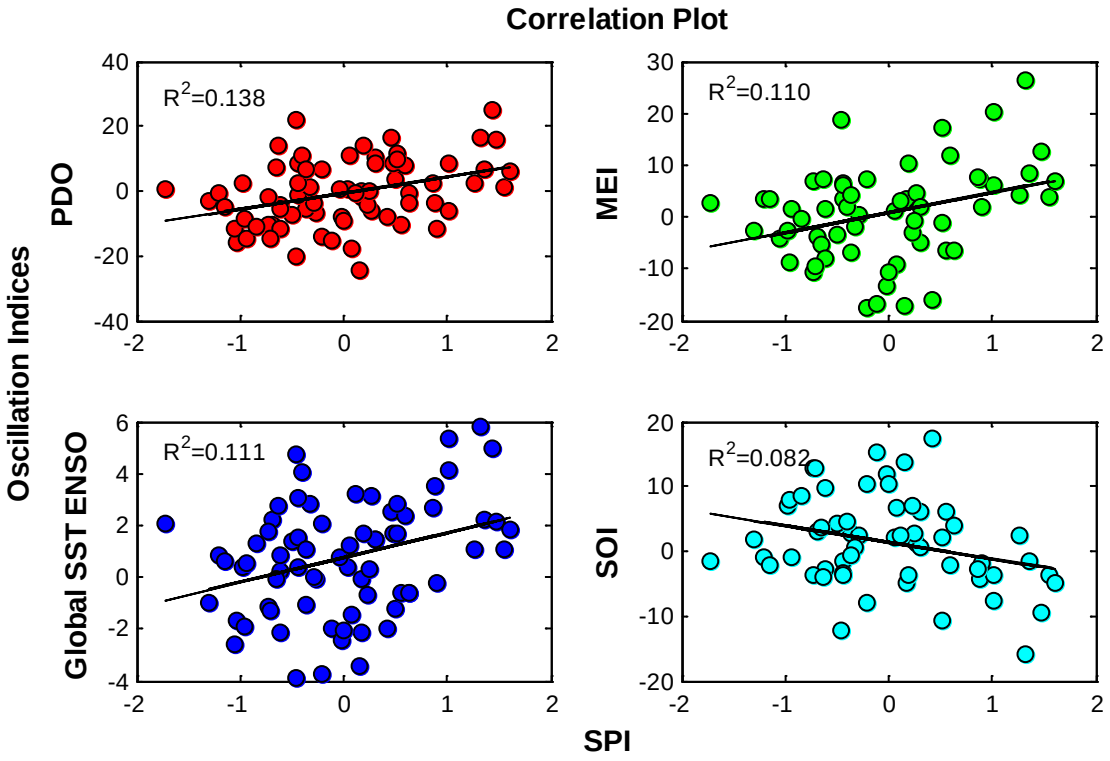

Figure C - 2: Correlation between Standardized Precipitation Index and Climate Indices

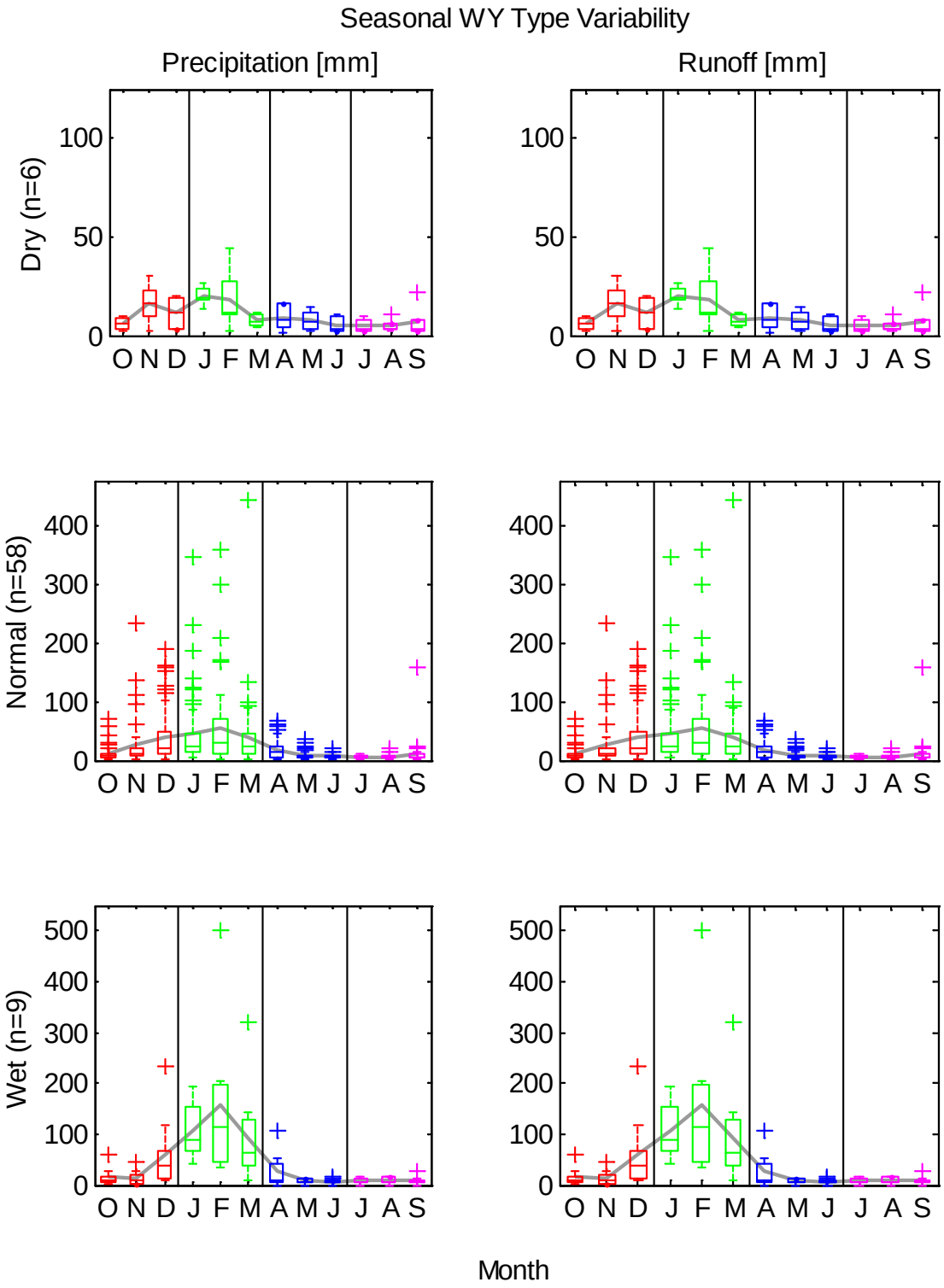

Figure C - 3: Annual Precipitation and Runoff Cycles based on the Standardized Precipitation Index (SPI) Wateryear Classification (Dry, Normal, or Wet)
(Barplots represent the distribution and the line represents the monthly mean)

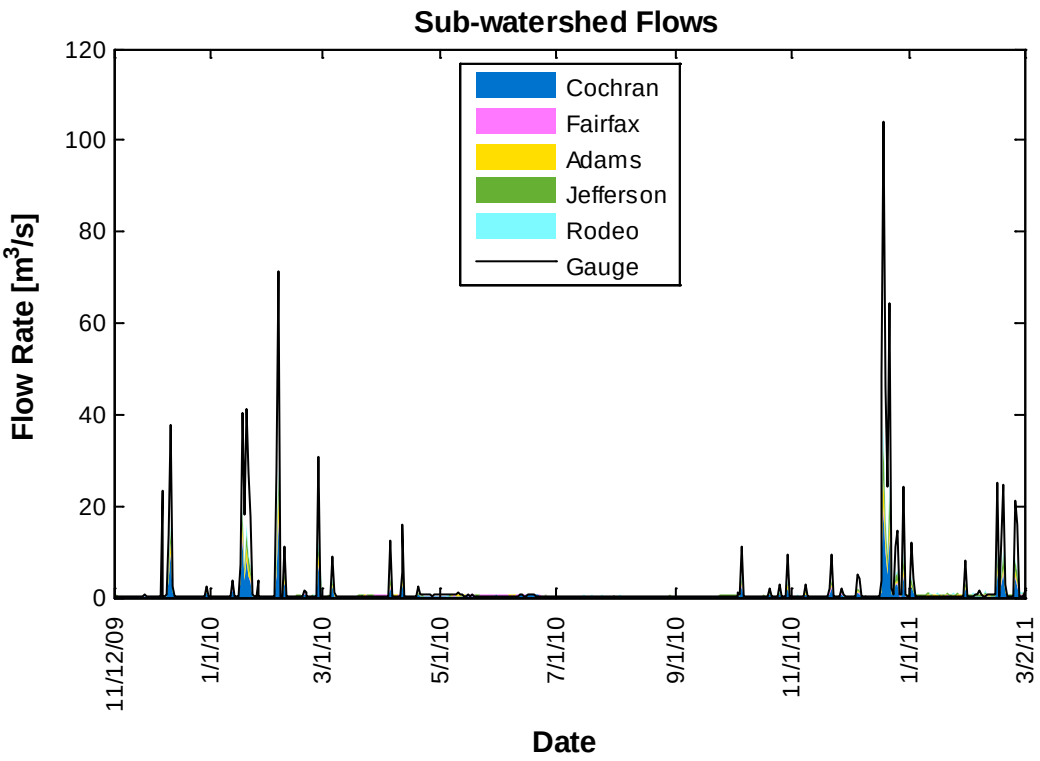

Figure C - 4: Time-series of Sub-watershed Flows (November 12, 2009 to March 2, 2011)

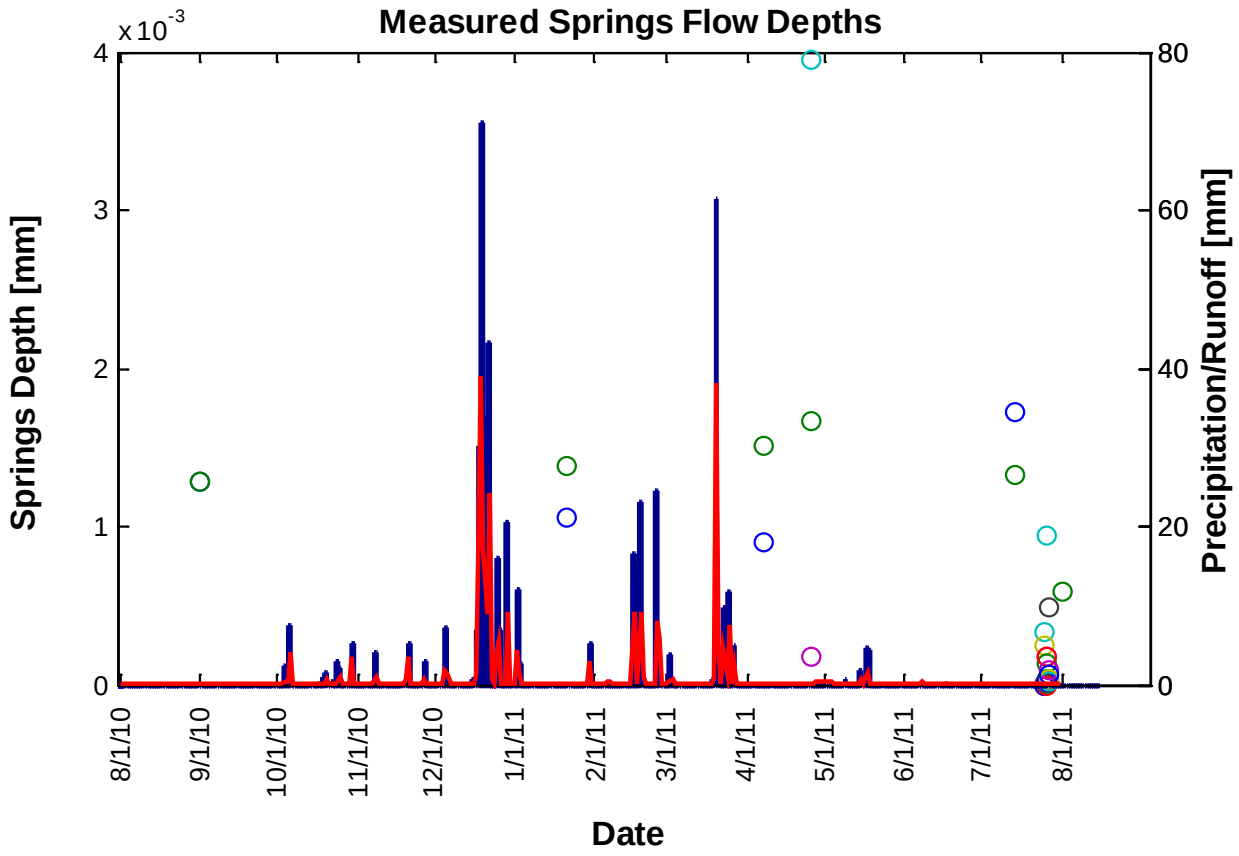

Figure C - 5: Measured Spring Flows relative to Daily Precipitation and Discharge